Palaeogeography, Palaeoclimatology, Palaeoecology 485 (2017) 879–898

Contents lists available at ScienceDirect

Palaeogeography, Palaeoclimatology, Palaeoecology

journal homepage: www.elsevier.com/locate/palaeo

Stratigraphic evidence for Hirnantian glaciation in the Alborz Mountain Ranges, northeastern Iran

Mohammad Ghavidel-Syooki

Institute of Petroleum Engineering, University of Tehran, P.O. Box 11365/4563, Iran

ARTICLE INFO

Article history:
Received 7 December 2016
Received in revised form 31 July 2017
Accepted 2 August 2017
Available online 5 August 2017

Keywords:
Northeast Iran
Diamictites
Hirnantian
Chitinozoans
Gondwana

ABSTRACT

The author examined the high-latitude Hirnantian diamictites of the Ghelli Formation and the early Silurian olive-gray shales of the Niur Formation exposed in the northeastern Alborz Mountains, Iran. These 404 m thick glacial deposits can be divided into three progradational-retrogradational cycles, each potentially controlled by the regional advance and retreat of the Hirnantian ice sheet. The glaciated source area was west of the study area, in the Arabian Shield region, where numerous tunnel valleys have been reported. Time calibration was performed based on a high-quality biostratigraphic control, mainly derived from the chitinozoan biozones *Tanuchitina fistulosa*, *Acanthochitina barbata*, *Armoricochitina nigerica*, *Ancyrochitina merga*, *Tanuchitina elongata*, *Spinachitina oulebsiri*, and *Spinachitina fragilis*. The land-derived miospores present in most chitinozoan assemblages, often abundant, seem associated with global sea-level changes during the Late Ordovician glaciation. The Ghelli Formation's high abundance of terrestrial miospores and low abundance of marine palynomorphs suggests its deposition in a shallow marine environment. Additionally, rhythmic bedded tidalites of claystone and sandstone indicate the growth of early land plants producing cryptospores on adjacent flooded areas. Based on marine palynomorphs (chitinozoans and acritarchs), the northeastern Alborz Mountains glacial deposits were dated as Hirnantian; the Niur Formation was assigned to the earliest Llandovery (Rhuddanian). Glacial deposits and marine palynomorphs suggest the presence of Hirnantian ice caps in the Alborz Mountains, at the margin of the Arabian Plate, and indicate the peripheral extension of the Late Ordovician ice sheet. Several biostrome beds forming pelmatozoan-bryozoan mud-mounds, mainly comprising bryozoans, echinoderms, tentaculites, and subordinate trilobites, were found in the glacial deposits of the Ghelli Formation, suggesting carbonate deposition during the Hirnantian. These carbonate beds are not related to the Boda warming event, which happened over the Gondwana landmass in the Katian interval; the glacial deposits of the Alborz Mountain Ranges are thus not correlated to those of the Gondwana paleocontinent. Climatic amelioration is more likely than local reduction of clastic input to be responsible for the biostrome beds in the Glacial Member of the Ghelli Formation, namely a short-lived episode of global warming during the Hirnantian interval (the Milankovitch cycles). Four new chitinozoan species, namely *Armoricochitina persianense* n. sp., *Tanuchitina alborzensis* n. sp., *Spinachitina iranense* n. sp., and *Hyalochitina jajarmensis* n. sp., are described and illustrated. Biometric data are also provided for the Iranian *S. oulebsiri* and *A. nigerica*.

1. Introduction

There is evidence of a widespread ice sheet over the Gondwanan supercontinent at the latest Ordovician (Hirnantian age). During a relatively short time (1–2 myr, Webby et al., 2004; 1.3–1.5 myr, Cohen et al., 2016), glaciers reached Gondwana sedimentary basins, resulting in extensive glacial deposits (Ghienne et al., 2007; Hirst et al., 2002; Le Heron and Craig, 2008; Vaslet, 1990). Some authors (see supplementary reference list S13, Brenchley et al., 1994; Sutcliffe et al., 2000) considered that this short period corresponded entirely to the Late Ordovician glaciation itself, whereas others regarded it as the period of maximum Gondwana glaciers, which extended throughout the early Silurian (Díaz-Martínez and Grahn, 2007).

The well-known glacial diamictites in South America (Zapla Formation) were assigned to the lower Silurian by Díaz-Martínez and Grahn (2007) and recently reinvestigated by Benedetto et al. (2015). Based on the in situ shelly fauna found in the glacial diamictites at the upper part of the Zapla Formation and on its chitinozoan and acritarch assemblages, this formation in northwestern Argentina was assigned to the Hirnantian instead of lower Silurian (Benedetto et al., 2015). This finding suggests that Gondwana glaciers disappeared at end of the Hirnantian age, although several authors reported a glaciation before the Hirnantian climax (e.g., Cherns and Wheeley, 2009 and references

E-mail address: mghavidel@ut.ac.ir.

http://dx.doi.org/10.1016/j.palaeo.2017.08.004

therein). According to these authors, an earlier Paleozoic glaciation might have been initiated as early as the base of the Katian (Dabard et al., 2015).

In the Middle East, Upper Ordovician glacial deposits have been recorded from the Arabian Peninsula (Clark-Lowes, 2005; McClure, 1978; Vaslet, 1990; McGillivray and Husseini, 1992; Melvin, 2015; Senalp and Al-Laboun, 2000) and neighboring countries, such as Jordan (Abed et al., 1993; Armstrong et al., 2009; Turner et al., 2005), Turkey (Ghienne et al., 2007; Monod et al., 2003) and Iran (Ghavidel-Syooki et al., 2011;). However, the peripheral extension of the Hirnantian ice sheet in the Arabian margin of Gondwana is still controversial. The Hirnantian tunnel valley networks differentiate the areas closest to the ice sheet center, such as Algeria, Arabia, Jordan, Libya, and Mauritania (Armstrong et al., 2009; Ghienne, 2003; Ghienne et al., 2007; Hirst, 2015; Le Heron et al., 2004), from 'ice-marginal areas', such as Morocco, Turkey, and Iran (Ghavidel-Syooki et al., 2011; Le Heron et al., 2007; Monod et al., 2003). Le Heron and Dowdeswell (2009) argued that several ice sheets rather than a continuous ice sheet developed throughout North Gondwana, including North Africa, Arabian Plate, South Africa, and South America. Some satellite ice caps on upland areas have been recognized in platforms fringing North Gondwana during the Hirnantian (e.g., Álvaro and Van Vliet-Lanoë, 2009; Le Heron et al., 2007), but no data are yet available for the Iranian Platform fringing the Arabian Plate.

Ghavidel-Syooki et al. (2011) reported high-latitude Hirnantian diamictites (Dargaz Formation) and lower Silurian kerogenous black shales (Sarchahan Formation) from the Zagros Mountains in Kuh-e Faraghan, northern Bandar Abbas, northern Persian Gulf. After this discovery, the author reinvestigated the Ordovician rock units in the Alborz Mountains to detect Hirnantian glacial deposits, which resulted in the first report of Hirnantian diamictites from this area. Here, glacial deposits are 404 m thick and include 40 m sandstone in the upper part of the Shale and Sandstone Member, the entire Mélange Member of the Ghelli Formation, and the Shale Member of the Niur Formation in the stratotype area (Fig. 1). Based on the available data regarding the development of a shifting Gondwanan ice cap (Ghienne, 2003 and references therein), glacial erosion and eustatic sea level change have resulted in incomplete Upper Ordovician successions (Paris et al., 1995) in northern Gondwana. However, in the northeastern Alborz Mountains (Kopeh-Dagh region), there is an almost complete Upper Ordovician outcrop in the stratotype of the Ghelli Formation (Fig. 2), comprising pre-glacial, glacial, and post-glacial marine deposits. Because these sequences have favorable lithologies for palynological investigations, the lower Paleozoic rock units of the study area were sampled several times for chitinozoan biozonation (Fig. 2). Thus, the present study aimed to: (i) analyze Upper Ordovician glacial deposits in the Alborz Mountains, (ii) establish regional correlations, and (iii) determine the age of these glacial deposits using biocomponents from the study area.

2. Geological setting and lithostratigraphy

The study area, Ghelli village, is located at the western part of Kuh-e Saluk, approximately 55 km southwest of Bojnourd city (Fig. 1). A thick lower Paleozoic sequence is well developed in this area, and it comprises the Mila, Lashkarak, Ghelli, and Niur formations in ascending stratigraphic order (Fig. 2). The Ghelli area is part of the northeastern (NE) Alborz Mountain Ranges (Kopeh-Dagh Region), and rock units extend toward the southern and eastern parts of the Caspian Sea. The Mila Formation consists mainly of limestone, with poorly preserved brachiopods and trilobites. Based on its stratigraphic position (Afshar-Harb, 1979) and index acritarch taxa (see supplementary reference list S13, Ghavidel-Syooki, 2000) it was assigned to the Middle and Upper Cambrian. The lower contact of the Mila Formation is not clear, due to a fault, but its upper contact is conformable with the Lashkarak Formation, which is 250 m thick and consists of olive-gray shales with stringers of rubbly limestone. The lower and upper contacts of the Lashkarak Formation are conformable with the underlying and overlying formations and, based on its acritarch assemblage zones, this rock unit was assigned to the lower Ordovician (Ghavidel-Syooki, 2000).

2.1. Ghelli Formation

This formation was first named and introduced for Ordovician deposits in NE Alborz Mountains by Afshar-Harb (1979). It was named after Ghelli village, where the reference section is located (56°55′51.80″ E and 37°11′39.82″ N). In the type locality, the Ghelli Formation is 900 m thick (Afshar-Harb, 1979) and divided into three members, in the following ascending stratigraphic order:

2.1.1. Volcanic Member (equivalent to the Mélange Member in this study)

This member consists of pyroclastic elements and lava flow, mixed with sedimentary strata. The lower contact of this member is conformable with the Lashkarak Formation and its upper contact is disconformable with the Shale and Sandstone Member of the Ghelli

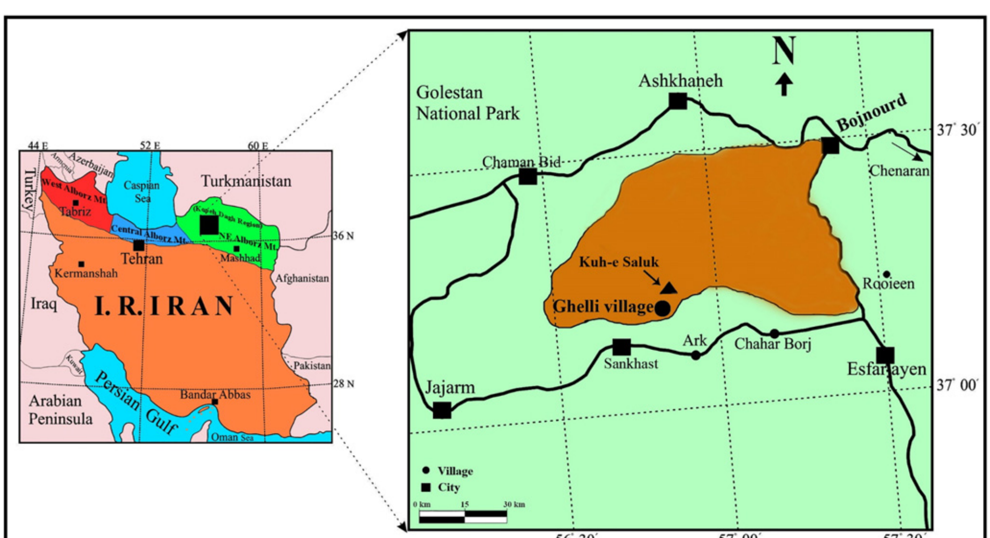

Fig. 1. Location map and connection of study area to major cities.

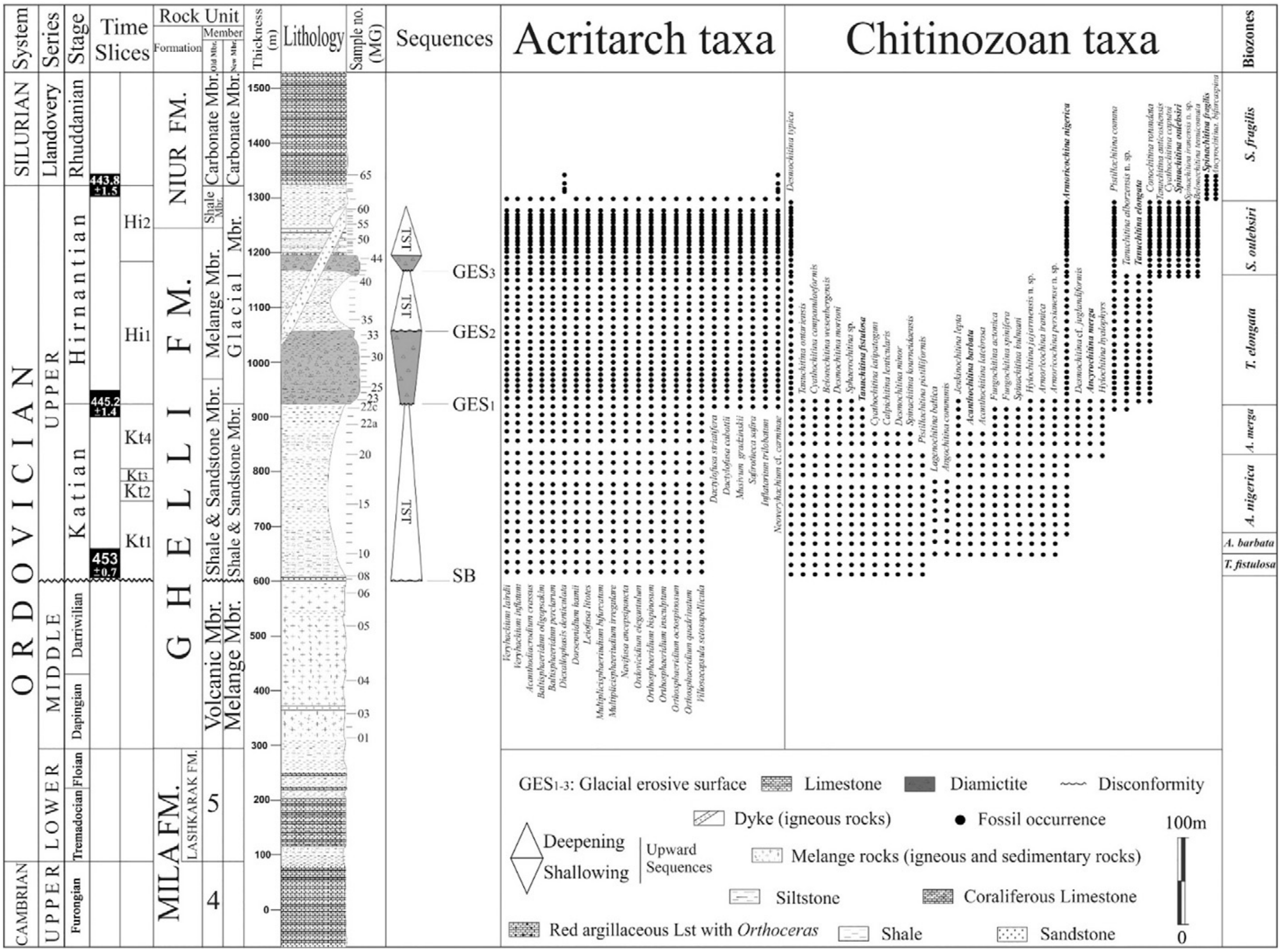

Fig. 2. Stratigraphic distributions of selected chitinozoan and acritarch taxa from the Ghelli and Niur formations in the stratotype section of Kuh-e Saluk, northeastern Alborz Mountains, Iran.

Formation (Fig. 2; see Supplementary data, Fig. S6, G). The Volcanic Member is 262 m thick and comprises (from base to top): 20 m light gray agglomerate, 121 m basic volcanic rock, 1 m light brown limestone and gray shale, 20 m basic volcanic rock, 20 m biosparite (dark gray and sandy limestone with thin layers of calcareous shale), 30 m dark brown and green sandstone (coarse-grained, poor to medium sorted, and cross-bedded in the lower part and graded in the top), 50 m dark green basic volcanic rock, 0.2 m red-brown highly fossiliferous shale, and 0.3 m light buff fossiliferous limestone (Afshar-Harb, 1979) (Fig. 3, D). Based on marine palynomorph (acritarch taxa) and brachiopod fauna, this member of the Ghelli Formation was assigned to the Middle Ordovician (Ghavidel-Syooki, 2000).

2.1.2. Shale and Sandstone Member

This member is 412 m thick and overlain by the Mélange Member. From base to top, this member consists of 2 m unsorted bioclastic wackstone and packstone (red colored argillaceous bearing straight orthoceras), 370 m alternating greenish-gray, non-calcareous silty and highly micaceous shale and greenish-gray, non-calcareous, highly micaceous sandstone, and 40 m light greenish-gray sandstone, well sorted, and slightly calcareous in some parts (Afshar-Harb, 1979). In the present study, microscopic investigations on the 2 m reddish-brown detrital carbonates of the basal part of this member revealed different bioclastic elements related to bryozoans, brachiopods, echinoderms, cephalopods, and gastropods (see Supplementary data, Fig. S5, A, B, C, D). The presence of these fossils and their location suggest a transgressive event at the onset of late Ordovician (upper Katian) and changes in the non-calcareous siliciclastic and rhythmic bedded tidalites of claystone and sandstone upward (Fig. 3, D). This reddish-brown, detrital carbonates fossiliferous unit is a good marker for correlating Upper Ordovician strata throughout NE Alborz Mountains (e.g., Fazel Abad area, southeastern Caspian Sea; Ghavidel-Syooki, 2016b) and the central Alborz Range (e.g., northwest Shahrud city; see supplementary reference list S13, Ghavidel-Syooki, 2006). Most of this member of the Ghelli Formation (370 m out of 412 m) comprises thin-bedded, rhythmic siliciclastic sediments and coarsening-upward, which contain ichnofossils such as *Cruziana*, *Rusophycus*, *Lockeia*, *Bifungites*, *Chondrites*, *Planolites*, *Bifasciculus*, *Monomorphichnus*, *Isopodichnus*, *Cochlichnus*, *Trichichnus*, and *Muensterria*, therefore corresponding to a neritic ramp condition (see supplementary reference list S13, Bargrizan, 1998). The remaining 40 m of this member is gray sandstone interbedded with thin-bedded shales, which contain cephalopods and dropstones, representing the beginning of marine glacial deposits in the Ghelli Formation (Fig. 3, C). Sedimentary textures such as coarsening-upward and Bouma's sequences are present in this sandstone unit (see Supplementary data, Fig. S5, F). Ten samples, representing dolomitic crinoid greywacke, dolomitic crinoid wackstone, and lithic greywacke, were prepared for a petrographic analysis. Echinoderm, crinoid, brachiopod, bryozoan, and trilobite remains were the most abundant bioclasts in the studied samples, indicating a shallow marine environment. However, a hiatus was found between the uppermost part of the Volcanic Member and the lowermost part of this member. This was due to the presence of a phosphoarenite bed, which marks the contact of both members together with reddish-brown detrital carbonates (Fig. 3, D; see Supplementary data, S5, A, B). On the other hand, the Sandbian chitinozoan *Lagenochitina ponceti* and *Lagenochitina deunffi* and lower Katian *Jenkinochitina tanvillensis* and *Belonechitina robusta* biozones, which encompass the whole Sandbian and lower Katian stages, were not recorded below the first appearance datum (FAD) of the *Tanuchitina fistulosa* biozone (Fig. 2).

2.1.3. Mélange Member (equivalent to part of the Glacial Member in this study)

This member is 224 m thick and consists of a syndeposited mélange of greenish-gray silty shale, siltstone, and sandstone, grading to a normal shale sequence near the top (Afshar-Harb, 1979; Ghavidel-Syooki, 2000). J. J. Chateauneuf studied this member of the Ghelli Formation for palynomorphs and J. G. Jenny studied a few samples from the Niur Formation for brachiopods (Afshar-Harb, 1979 and references therein). Thus, based on paleontological data, the Ghelli Formation was assigned to the Upper Ordovician and the Niur Formation to the lower Silurian. In the present study, glacial-related strata comprise the upper part of the Shale and Sandstone Member (40 m), the Mélange Member of the Ghelli Formation (224 m), and the Shale Member of the Niur Formation (140 m). Therefore, the glacial deposits of the study area were named “Glacial Member,” and this is divided into four informal subunits: lower diamictite, middle shale, upper diamictite, and upper heterolithic; the latter is associated to igneous sill near the top (Figs. 2, 3, A, B).

The Glacial Member is 404 m thick and it is characterized by scattered granular, pebble-sized to outsized clasts, which are either isolated or chaotically clustered, and embedded in a greenish-gray clayey siltstone matrix (Fig. 4, A, B, C, E, F, G; see Supplementary data, Fig. S5, E, H and Fig. S6, D). The sandstone bodies of this member are medium–thick bedded without cross-lamination (Fig. 4, D; see Supplementary data, Fig. S5, F) and load and flute casts, indicating a range of north to northeast-directed palaeocurrents (see Supplementary data, Fig. S6, B). Thin-sections revealed a mixture of unsorted, fine–medium grained sandstone with relatively high mud content, occasionally preserving granule-sized feldspars and quartzite granules floating in a fine-grained matrix (Fig. 5, D). Outsized clasts embedded in massive diamictites represent the settling of suspended fine material and the release of coarser dropstones from icebergs in the vicinity of a calving front (Fig. 4, A, B). Weakly developed lamination may reflect episodic current activities resulting from storms, turbidity, or wave-influenced processes. Dropstones are not striated and range from 1 cm to more than 1 m (Fig. 4, A, B; see Supplementary data, Fig. S5, E). The proportions of clay, silt, and sand also vary in Bouma sequences (Fig. 4, D). Calcareous fauna had not yet been recorded from the lower unit of the Glacial Member of the Ghelli Formation, but the present study allowed recognizing cephalopods (see Supplementary data, Fig. S5, H), tentaculites (see Supplementary data, Fig. S5, G), crinoids (see Supplementary data, Fig. S5, D), bryozoans (see Supplementary data, Fig. S6, H), and trilobite fragments (Fig. 5, E). These are associated with the *Tanuchitina elongata* chitinozoan biozone that corresponds to the early Hirnantian (Fig. 2). This unit changes into a shaly facies, which is overlain by the upper unit of the Glacial Member, and mainly consists of gray-black shale and a few dropstones (Fig. 4, G). An in situ single lenticular bryozoan patch was also found in this unit (see Supplementary data, Fig. S6, H).

The upper diamictite unit is characterized by the appearance of clifforming dropstones ranging from cobbles to granules (Fig. 4, H), and changes upward alternating black papery shale and biostrome beds containing common echinoderms (*Caryocrinites* sp., *Heliocrinites* sp., and *Hemicosmites* sp.; see Supplementary data, Fig. S6 and S7), abundant brachiopods (see Supplementary data, Fig. S6, A, C), extremely abundant bryozoans (Fig. 5, F, G, J; see Supplementary data, Fig. S7, B, D, F, G, H), a few tentaculites (see Supplementary data, Fig. S7, B), a few cephalopods (see Supplementary data, Fig. S7, E), and very rare trilobites (see Supplementary data, Fig. S7, A). These coquina or biostrome beds are recorded for the first time from the Upper Ordovician (Hirnantian) in Iran, and are not equivalent to those of the Katian age in the North Gondwana Domain. These Ashgill-aged carbonate-siliciclastic shallow-water sediments have been recorded throughout northern Gondwana during the periglacial episode in the Katian (Fortey and Cocks, 2013) and may have preceded the latest Ordovician glacial event in the Hirnantian (Vennin et al., 1998). Carbonate deposits include bryozoan biostromes, Djeffara Formation in Libya (see Supplementary reference list S13, Bergström and Massa, 1991), bryozoan limestones, Khant-el-Hajar in the Moroccan Anti Atlas (see supplementary reference list S13, Destombes et al., 1985; Loi et al., 2010), and Cystoid limestone in the Iberian Chains, NE Spain (Vennin et al., 1998). Detailed systematic studies on the echinoderms (Chauvel et al., 1975; Chauvel and Le Menn, 1979), brachiopods (see supplementary reference list S13, Villas, 1985), conodonts (Carls, 1975), and trilobites (Hammann, 1992) found in these carbonate deposits and on their sequence

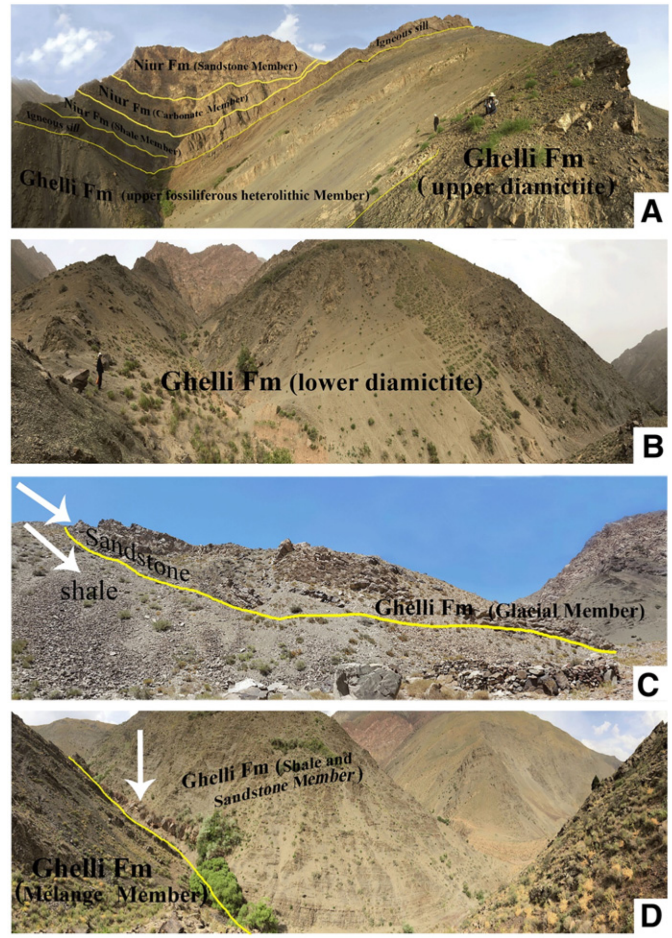

Fig. 3. A. Illustration of the contact between the Ghelli and Niur formations and of the upper diamictite and calcareous dark gray shale with thin-bedded biostrome beds; B. Extension of the lower diamictite of the Glacial Member of the Ghelli Formation in the stratotype section; C. Contact between the Shale and Sandstone Member and the Glacial Member of the Ghelli Formation; D. Illustration of the Mélange and Shale and Sandstone members of the Ghelli Formation in the stratotype section of Kuh-e Saluk. Scale is the same in A, B, and C. Field photos from D to A indicate the members of the Ghelli Formation in ascending stratigraphic order.

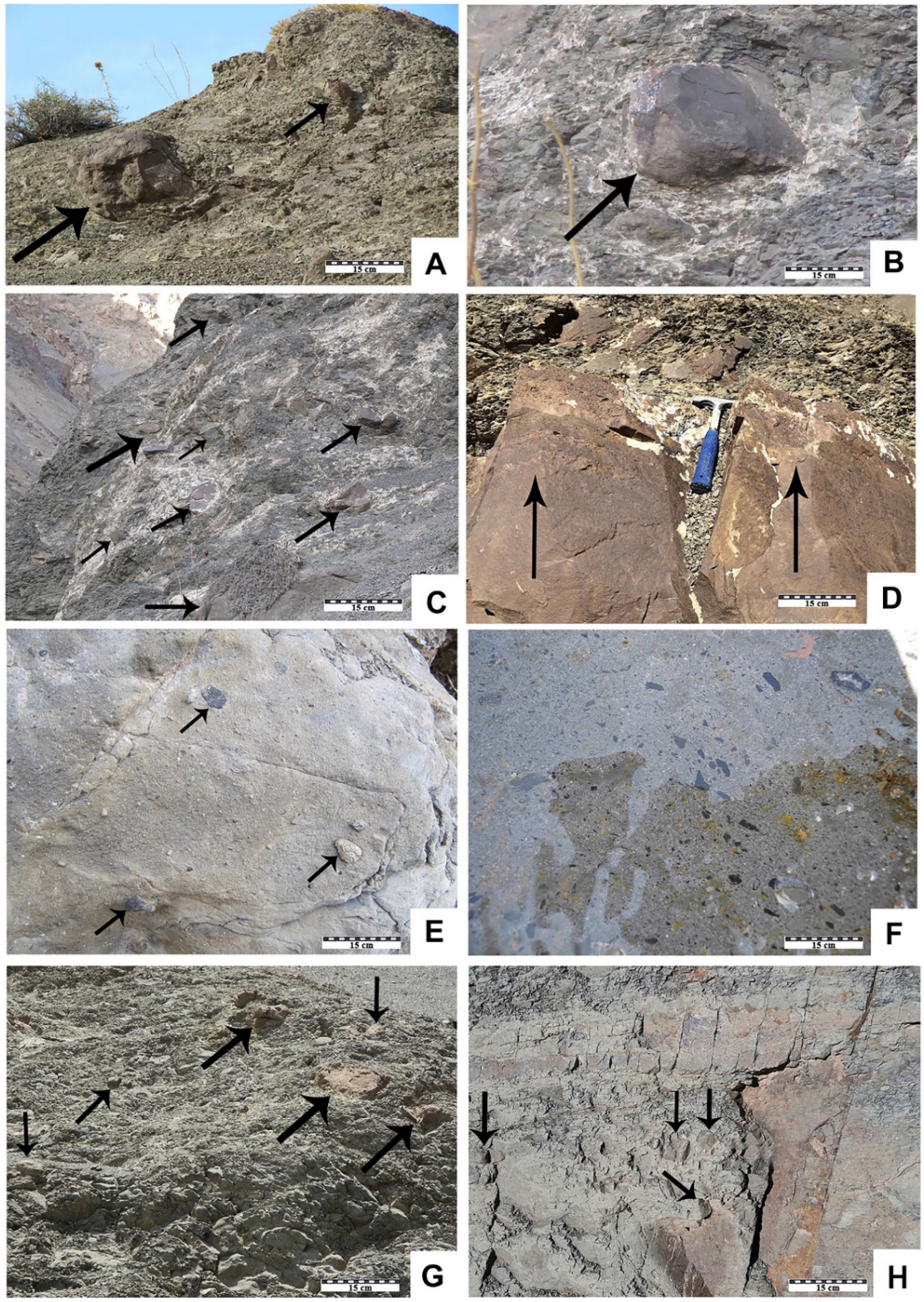

Fig. 4. A, B, G. Quartzitic lonestone embedded in mudstone (arrows indicate lonestones) in the lower unit of the Glacial Member of the Ghelli Formation in the stratotype section of Kuh-e Saluk; C. Dropstones of various sizes in the lower unit of the Glacial Member (arrows indicate dropstones); D. Coarsening upward cycles (arrows indicate the Bouma sequence) in the lower unit of the Glacial Member (scale bar = 15 cm); E, F. Diamictite with dropstones of various sizes in the silty shale of the lower unit of the Glacial Member (arrows indicate dropstones); H. Dropstones of different sizes (granule, pebble, and cobble) in the upper unit of the Glacial Member (arrows indicate dropstones).

stratigraphy allowed assigning them to the Ashgill age (Katian) in the Northern Gondwana Domain, whereas Iranian biostrome beds fall into the *T. elongata* and *S. oulebsiri* biozones of the Hirnantian age. Therefore, except for the well-known chitinozoan biozones from the Ghelli Formation, these fossiliferous biostrome beds cannot be used for correlating the Upper Ordovician strata in Iran to the North Gondwana Domain.

2.2. Niur Formation

This formation is 675 m thick in the Ghelli area and, in ascending stratigraphic order, comprises the Shale Member (140 m), the Carbonate Member (145 m; with trilobites and brachiopods), and the Sandstone Member (390 m; Fig. 3, A; Fig. 12). The lower contact of this formation is conformable with the Ghelli Formation and channeled conglomerates of the Padeha Formation (Upper Devonian) mark the top of its erosive surface. Several specialists (Afshar-Harb, 1979 and references therein; see supplementary reference list S13, Brice et al., 1973) studied the coral, trilobite, and brachiopod faunas from the fossiliferous Carbonate Member of the Niur Formation. Based on index fossils, it has been assigned to the lower–middle Silurian (Llandovery-Wenlock) and palynological investigations carried out on the Niur and Ghelli formations of Pelmis Gorge, Alborz Mountain Ranges (Ghavidel-Syooki,

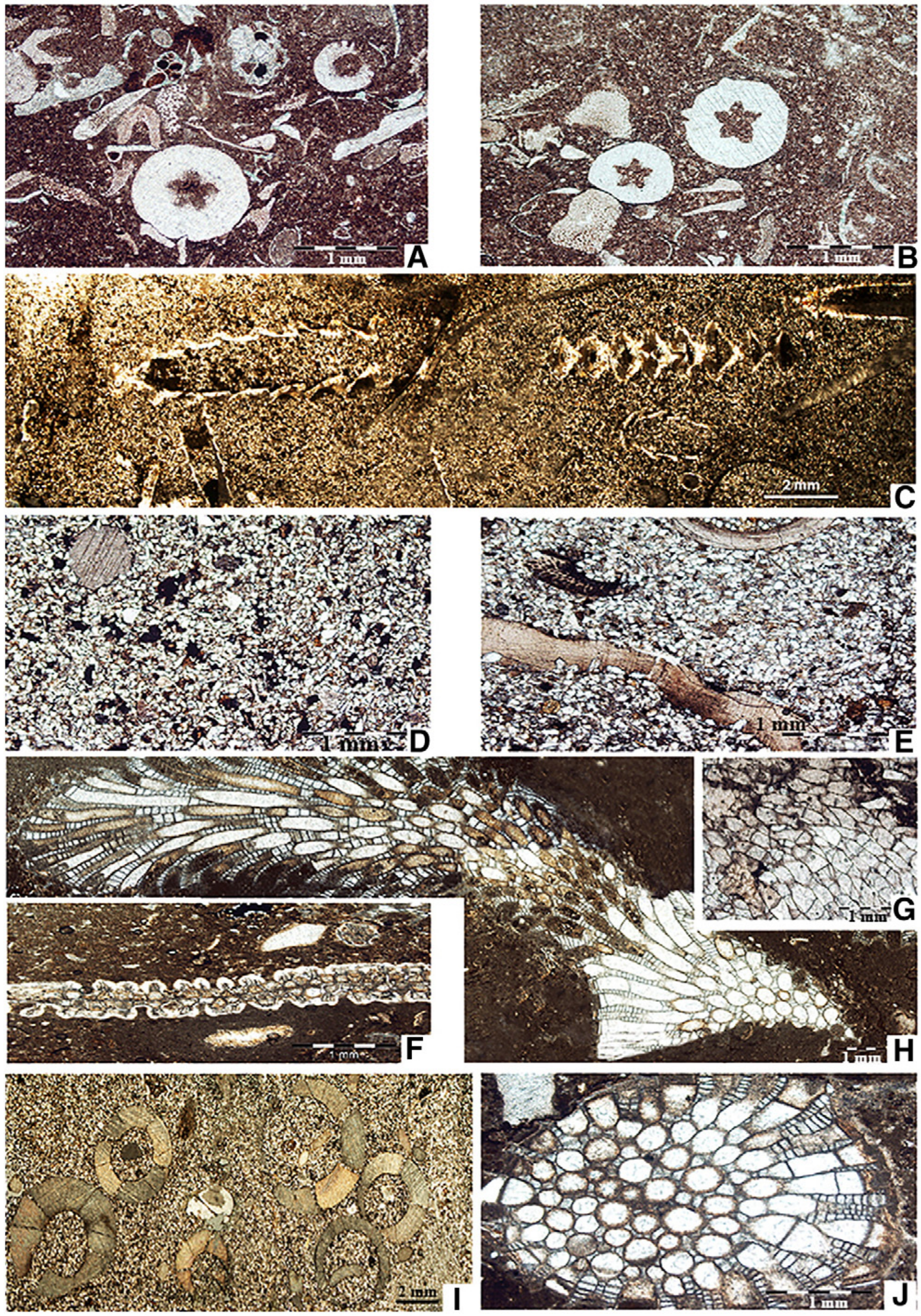

Fig. 5. A, B. Plane-polarized photomicrograph of bryozoan-crinoid floatstones surrounded by a micritic matrix of reddish brown detrital carbonates at the basal part of the Shale and Sandstone Member of the Ghelli Formation (scale bar = 1 mm); C. Plane-polarized photomicrograph of tentaculites surrounded by a micritic matrix at the lower unit of the Glacial Member (scale bar = 2 mm); D. Plane-polarized photomicrograph of massively stratified diamictite at the lower unit of the Glacial Member (scale bar = 1 mm); E. Plane-polarized photomicrograph of massively stratified diamictite and bioclasts (scale bar = 1 mm); F, G, J. Plane-polarized photomicrograph of longitudinal (F) and transversal (G, J) sections of bryozoan bafflestone surrounded by a micritic matrix at the upper unit of the Glacial Member (scale bar = 1 mm); H. Plane-polarized photomicrograph of tentaculites in the muddy texture of the lower unit of the Glacial Member (scale bar = 1 mm); I. Plane-polarized photomicrograph of crinoids at the lower unit of the Glacial Member (scale bar = 2 mm).

2000; Ghavidel-Syooki and Vecoli, 2007; Ghavidel-Syooki, 2016a) also assigned this member to the lower Silurian (Llandovery). Although no fossils were found in the Shale Member of the Niur Formation by Afshar-Harb (1979), this author tentatively assigned it to the lower Silurian by means of its stratigraphic position (Fig. 2).

3. Biostratigraphic control

In the present study, both the Ghelli and Niur formations were systematically sampled to check for a possible diachronism in their lithostratigraphic contacts. Most studied samples from both formations (Shale and Carbonate members of the Niur Formation) contained well-preserved and abundant palynomorphs including acritarchs, chitinozoans, scolecodonts, and miospores. Miospores and acritarchs ranged from yellow to orange-brown indicating an intermediate degree of thermal maturity (see Supplementary data, Fig. S12) in this part of the Alborz Mountains. All samples and slides related to this study are deposited in the Iranian Natural History Museum, Department of Organization Environment (DOE) under accessions MG-01 to MG-65 (Fig. 2).

Thirty-eight chitinozoan species (four of which are new), belonging to 18 genera, and 18 acritarch species, belonging to 10 genera, were identified and their distributions are plotted in Fig. 2. Scanning electron and transmitted light microphotographs were prepared for selected acritarch and chitinozoan taxa and are presented in Figs. 6–11. The acritarch taxa discussed and illustrated here were designated form species and form genera under the provisions of the International Code of Botanical Nomenclature (Greuter et al., 1994; see Supplementary data, S4), and are arranged alphabetically by genera, under the informal *incertae sedis* "acritarch" group. Chitinozoans were treated under the provision of the International Code of Zoological Nomenclature (Paris et al., 1999). The classification adopted here is based on Paris et al., 1999 (see Supplementary data S2 and S3).

3.1. Chitinozoan biostratigraphy

The identified chitinozoan fauna allowed recognizing seven biozones in the Ghelli and Niur formations, all well-known from the North Gondwana Domain. These chitinozoan biozones and their biostratigraphic age are discussed below in ascending stratigraphic order

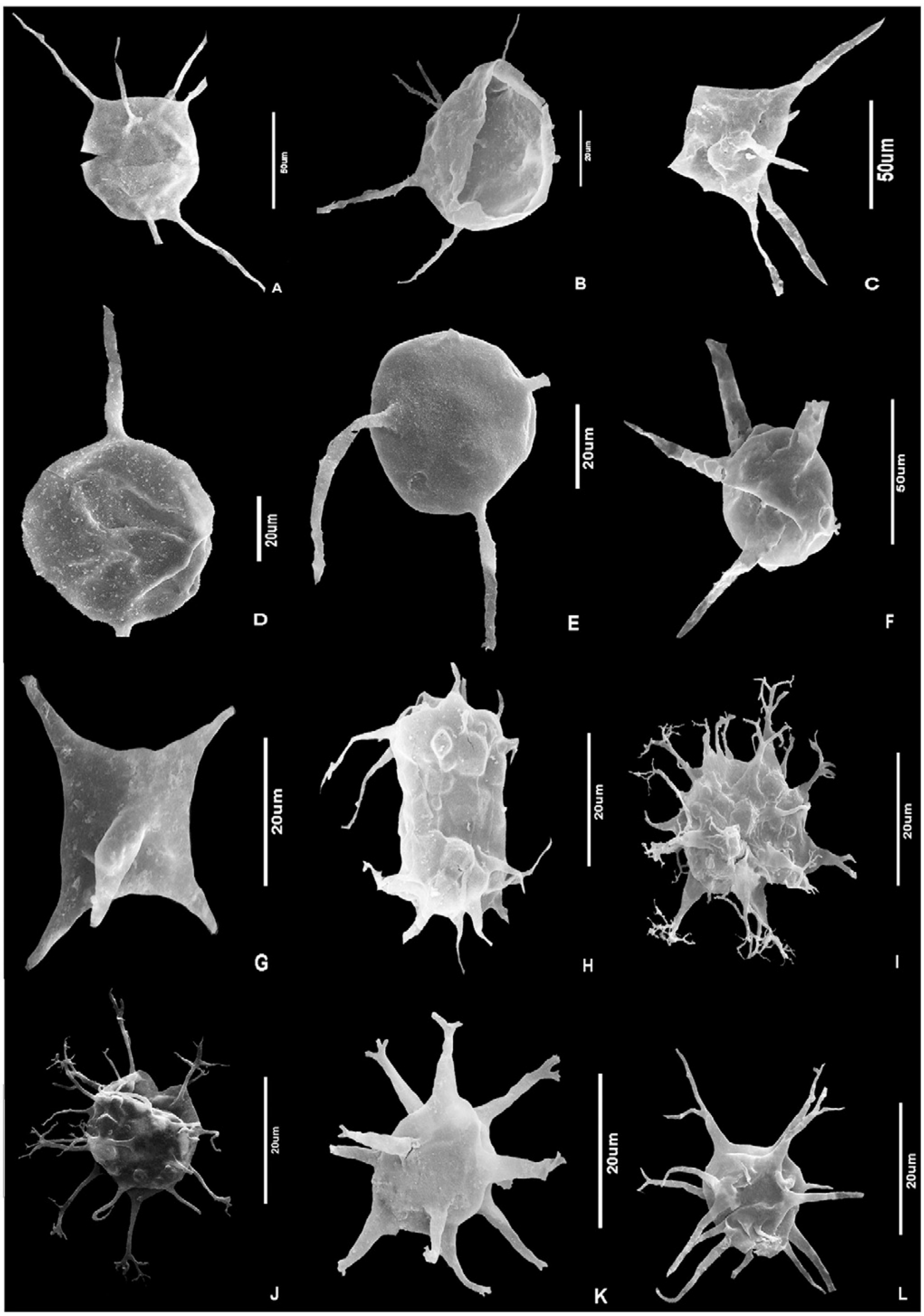

Fig. 6. A, B. *Orthosphaeridium insculptum* (Loeblich, 1970); C. *Orthosphaeridium octospinosum* Eisenack, 1968; D. *Orthosphaeridium bispinosum* Turner, 1984; E. *Orthosphaeridium quadrinatum* (Burmann, 1970) Eisenack et al., 1976; F. *Baltisphaeridium perclarum* (Loeblich and Tappan, 1978); G. *Veryhachium inflatum* Hashemi and Playford, 1998; H. *Acanthodiacrodium crassus* (Loeblich and Tappan, 1978) Vecoli, 1999; I, J. *Multiplicisphaeridium irregulare* (Staplin et al., 1965); K. *Cheleutochroa* sp. aff. *venosa* Utela and Tynii, 1991; L. *Multiplicisphaeridium bifurcatum* (Staplin et al., 1965).

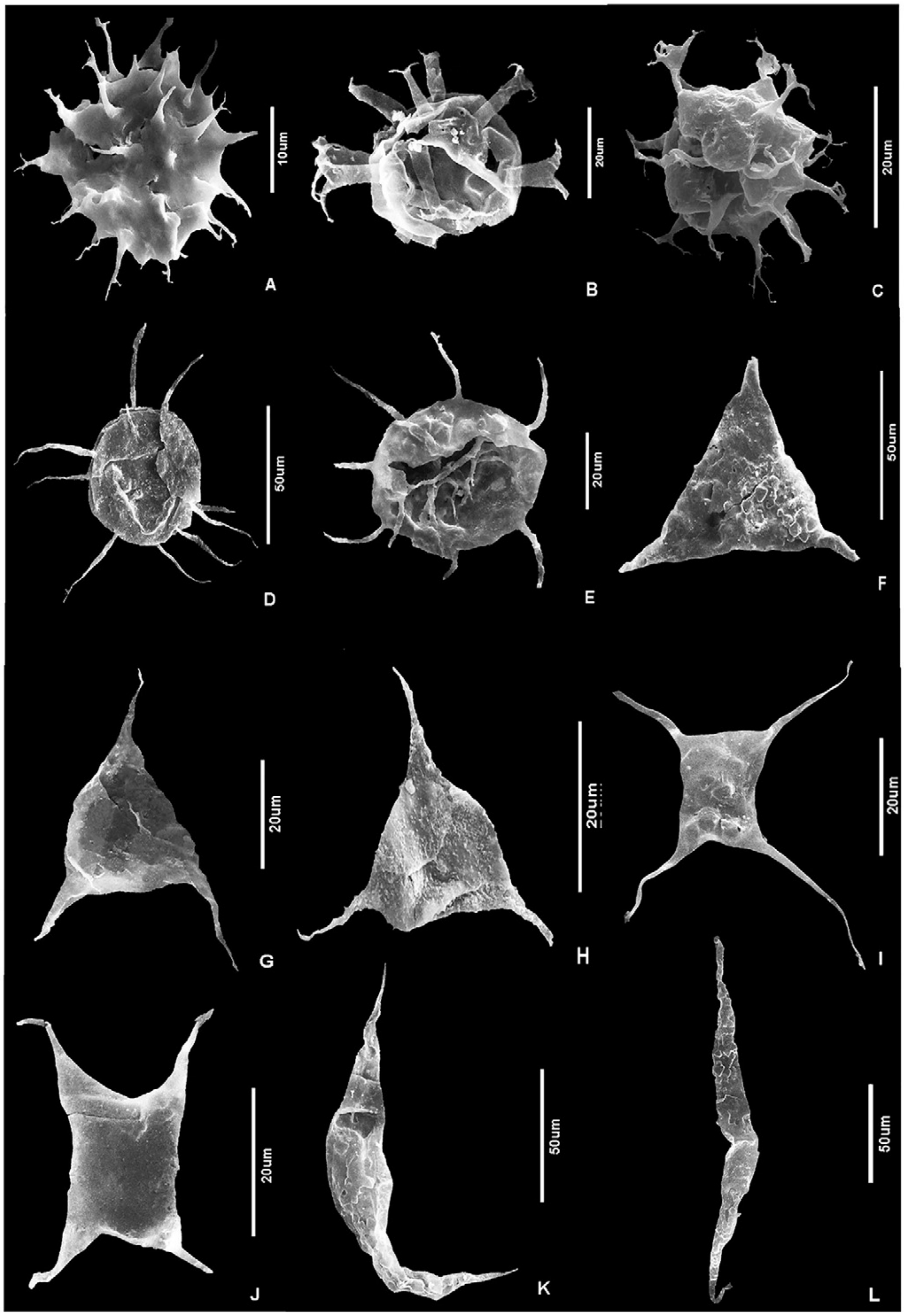

Fig. 7. A. *Multiplicisphaeridium bifurcatum* (Staplin et al., 1965); B. *Ordovicidium elegantulum* Tappan and Loeblich, 1971; C. *Multiplicisphaeridium irregulare* (Staplin et al., 1965); D, E. *Baltisphaeridium oligopsakium* (Loeblich and Tappan, 1978); F. *Veryhachium triangulatum* Konzalova-Mazancova, 1969; G. *Veryhachium trispinosum* (Eisenack) Deunff, 1954 ex Downie, 1954; H. *Villosacapsula setosapellicula* Loeblich and Tappan, 1976; I, J. *Veryhachium lairdii* (Deflandre) Deunff 1959 ex Downie 1959; K. *Dactylofusa striatifera* (Cramer and Diez, 1976) (Fensome et al., 1990); L. *Leiofusa litotes* Loeblich and Tappan, 1976.

(Abuhmida, 2013; Bourahrouh et al., 2004; Ghavidel-Syooki and Winchester-Seeto, 2002; Ghavidel-Syooki, 2008, 2016a, 2016b; Loi et al., 2010; Paris, 1996; Paris et al., 2000b, 2007, 2015; see Supplementary data, S2). Detailed descriptions and biometric data are provided only for the four new chitinozoan species, i.e., *Armoricochitina persianense* n. sp., *Tanuchitina alborzensis* n. sp., *Spinachitina iranense* n. sp., and *Hyalochitina jajarmensis* n. sp. Biometric data for *S. oulebsiri*, *S. fragilis*, and *A. nigerica* were obtained from published papers containing data from Iran, the Arabian Peninsula, and Libya (see Supplementary data, S3).

3.1.1. *Tanuchitina fistulosa* biozone

This biozone corresponds to the FAD of *T. fistulosa* (see supplementary reference list S13, Taugourdeau and de Jekhowskey, 1960) in the lowermost sample of the Shale and Sandstone Member of the Ghelli Formation (Fig. 2, MG-08), and extends to the succeeding biozones. *Tanuchitina fistulosa* was selected as the index species of the chitinozoan biozones from the Upper Caradoc in the Arabian Peninsula (Paris et al., 2000b) and North Gondwana Domain, immediately overlying the *Belonechitina robusta* biozone (lower Katian; Videt et al., 2010). There

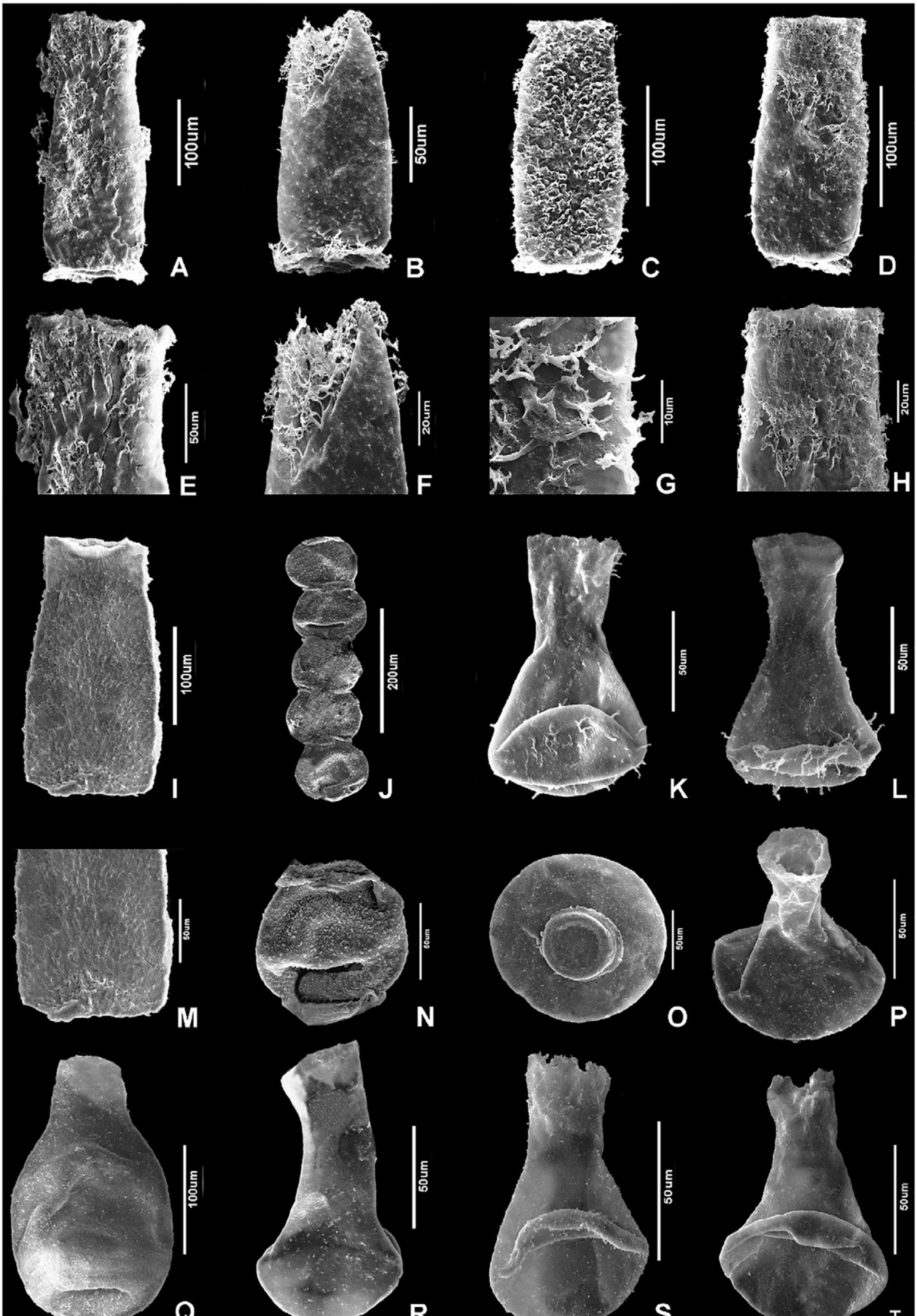

Fig. 8. A, E. *Acanthochitina barbata* Eisenack, 1931; B, F. *Acanthochitina barbata* Eisenack, 1931; C, G. *Acanthochitina barbata* Eisenack, 1931; D, H. *Acanthochitina barbata* Eisenack, 1931; I, M. *Acanthochitina latebrosa* Vanderbroucke, 2008; J, N. *Desmochitina mortoni* Al- Ghammari et al., 2010; K, L. *Angochitina communis* (Jenkins, 1967); O. *Calpichitina lenticularis* (Bouché 1965); P, T. *Euconochitina lepta* (Jenkins, 1970); Q. *Lagenochitina baltica* Eisenack, 1931; R. *Sphaerochitina* sp.; S. *Fungochitina spinifera* (Eisenack, 1932).

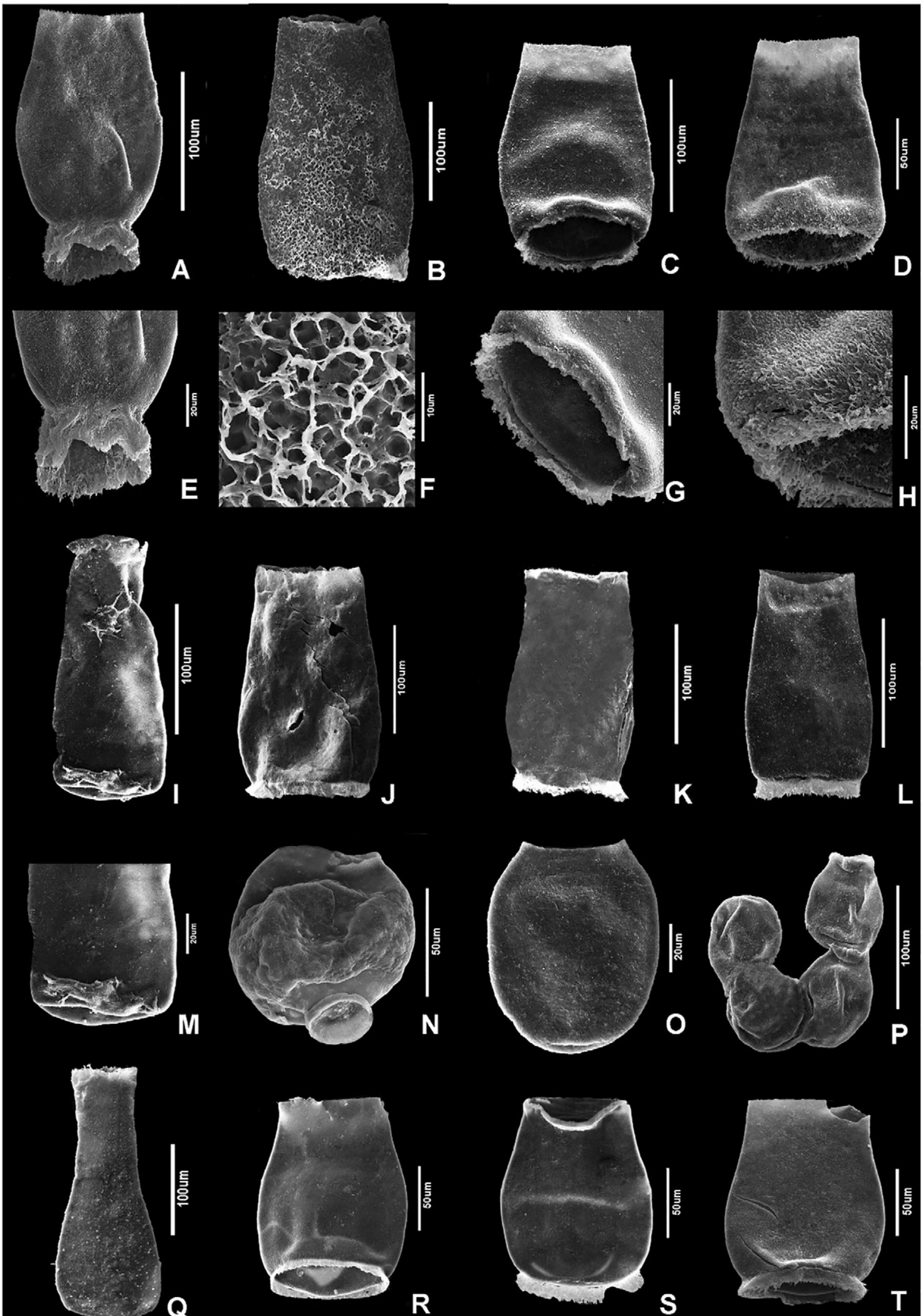
100um
A
100um
B
100um
C
50um
D
20um
E
10um
F
20um
G
20um
H
100um
I
100um
J
100um
K
100um
L
20um
M
50um
N
20um
O
100um
P
100um
Q
50um
R
50um
S
50um
T

is no data for delimiting the base of this biozone and its top can only be defined by the FAD of *Acanthochitina barbata* (in the Arabian Peninsula the chitinozoan *Armoricochitina* sp. aff. *fistulosa* is equivalent to *T. fistulosa*). Based on the absence of L. *ponceti* to *B. robusta* chitinozoan biozones and on comparisons to the chronostratigraphic chart of Videt et al. (2010), the basal part of the Shale and Sandstone Member of the Ghelli Formation was assigned to the uppermost Kt1 time slice of Katian stage (Fig. 2). This biozone is characterized by the co-occurrence of the chitinozoan taxa *Desmochitina typica*, *Tanuchitina ontariensis*, *Cyathochitina campanulaeformis*, *Belonechitina wesenbergensis*, *Desmochitina mortoni*, *Sphaerochitina* sp., *Cyathochitina latipatagium*, *Calpichitina lenticularis*, *Desmochitina minor*, *Spinachitina* cf. *kourneidaensis*, and *Pistillachitina pistillifrons*. Among these species, *C. lenticularis*, *D. typica*, *T. ontariensis*, *P. pistillifrons*, C. *latipatagium*, and *Spinachitina* cf. *kourneidaensis* are classical components of the Late Ordovician in the North Gondwana Domain (Ghavidel-Syooki and Winchester-Seeto, 2002; Ghavidel-Syooki et al., 2011; Ghavidel-Syooki, 2016a, 2016b; Molyneux and Paris, 1985; Oulebsir and Paris, 1995; Paris et al., 2015; see supplementary reference list S13, Al-Hajri, 1995). The remaining chitinozoan species, i.e., *D. minor*, *B. wesenbergensis*, *C. campanulaeformis*, and *D. mortoni* have a long range (Middle to Upper Ordovician) and are cosmopolitan (Achab, 1978; Jenkins, 1967; see supplementary reference list S13, Al-Ghammari et al., 2010; Al-Hajri, 1995; Eisenack, 1931, 1959; Grahn, 1981, 1984).

3.1.2. *Acanthochitina barbata* biozone

This biozone is marked by the FAD of *A. barbata* in the lower part of the Shale and Sandstone Member of the Ghelli Formation (Fig. 2, MG-10) and it extends to the succeeding biozones. Paris et al. (2000b) selected *A. barbata* as the index species of the biozone immediately succeeding the *T. fistulosa* biozone in the North Gondwana Domain. This biozone is characterized by the co-occurrence of the chitinozoan taxa *Euconochitina lepta*, *Acanthochitina latebrosa*, *Fungochitina actonica*, *Fungochitina spinifera*, *Spinachitina bulmani*, *Armoricochitina iranica*, *Hyalochitina jajarmensis* n. sp., *Armoricochitin*a *persianense* n. sp., *Lagenochitina baltica*, and *Angochitina communis*. All these chitinozoan species are within the Ashgillian stage (Abuhmida, 2013; Elaouad-Debbaj, 1984; Ghavidel-Syooki, 2000; Ghavidel-Syooki and Winchester-Seeto, 2002; Ghavidel-Syooki, 2008; Jenkins, 1967, 1970; Oulebsir and Paris, 1995; Paris, 1990; Van Nieuwenhove et al., 2006; Vandenbroucke et al., 2009; see supplementary reference list S13, Al-Hajri, 1995; Jansonius, 1964).

It should be noted that *A. latebrosa*, *H. jajarmensis* n. sp., and *A. persianense* n. sp., are recorded for the first time from the Upper Ordovician of Iran (Fig. 2, MG-10; see Supplementary data, S3). Furthermore, Al-Hajri (1995) and Paris (1990) found *E. lepta* (*Jenkinochitina lepta*) in the *A. nigerica* and *A. merga* biozones of the North Gondwana Domain. Paris et al. (1999) used L. *baltica* to link the chitinozoan biozonations of Laurentia and North Gondwana. Based on the age assignments adopted by Paris et al. (2000b) and Webby et al. (2004) for the *T. fistulosa* and the *A. barbata* biozones, respectively, the lowermost part of the Shale and Sandstone Member of the Ghelli Formation (between MG-08 and MG-10) is assigned to the late Caradoc–early Ashgill age. However, based on the absence of L. *ponceti* to *B. robusta* chitinozoan biozones and on comparisons with the chronostratigraphic chart of Videt et al. (2010), the basal part of the Shale and Sandstone Member of the Ghelli Formation was assigned to the middle (Kt2) to lowermost (Kt3) Katian stage (Fig. 2). Therefore, there is a hiatus between the Volcanic and the Shale and Sandstone Members of the Ghelli Formation, encompassing the Sandbian and lowermost part of Katian.

3.1.3. *Armoricochitina nigerica* biozone

This biozone is marked by the FAD of *A. nigerica* in the sample MG-13 of the Shale and Sandstone Member of the Ghelli Formation (Fig. 2), and extends to the succeeding biozones. To date, *A. nigerica* has only been recorded from the Late Ordovician in the North Gondwana Domain (Abuhmida, 2013; Al-Hajri, 1995; see supplementary reference list S13, Bouché, 1965; Bourahrouh et al., 2004; Ghavidel-Syooki, 2000; Ghavidel-Syooki and Winchester-Seeto, 2002; Ghavidel-Syooki, 2008; Ghavidel-Syooki et al., 2011; Ghavidel-Syooki, 2016a, 2016b; Le Hérissé et al., 2013; Le Heron et al., 2008; Molyneux and Paris, 1985; Oulebsir and Paris, 1995; Paris et al., 2000b, 2007, 2015). According to Paris (1990, 1996) and Bourahrouh et al. (2004), the *A. nigerica* biozone is a partial-range biozone comprising the stratigraphic interval between the last appearance datum of *A. barbata* and the FAD of *A. merga*, which is the index species of the succeeding biozone. The *A. nigerica* biozone is correlated to the upper part of the *Dicellograptus complanatus* graptolite zone of the British Standard (Paris, 1990, 1996; Webby et al., 2004), thus corresponding to the upper part of Kt3 to lower part of Kt4 time slices of the Katian (Videt et al., 2010). *Armoricochitina nigerica* has been reported in Katian and Hirnantian strata from numerous localities in North Africa (Morocco, Algeria, Tunisia, Libya, Niger, and Chad), Middle East (Iran, Arabian Peninsula, Syria, Iraq, and Turkey), and southern and central Europe (Spain, Portugal, France, Italy, and Czech Republic). This species is one of the key chitinozoan taxa defining the northern Gondwana paleobiogeographic province during the late Ordovician. The absence of *A. nigerica* in the United Kingdom and Belgium indicates that this species did not extend to the northern margin of the Rheic Ocean (Paris et al., 2015). Indeed, Vandenbroucke et al. (2009) suggested that *A. nigerica* distribution was latitudinally controlled and it could be regarded as a polar taxon. The *A. nigerica* biozone includes most species from the preceding biozones.

3.1.4. *Ancyrochitina merga* biozone

This biozone is characterized by the FAD of *A. merga* in samples MG-20 and MG-22C from the Shale and Sandstone Member of the Ghelli Formation (Fig. 2), and its top is marked by a glacial erosive surface (GES1) overlaid by glacial deposits. According to Paris (1990) and Bourahrouh et al. (2004), this biozone is an interval-range zone between the FAD of *A. merga* and the FAD of *T. elongata*, the index species of the succeeding biozone (Fig. 2). Paris (1990) and Bourahrouh et al. (2004) have discussed the biostratigraphic age of this biozone, suggesting a middle–upper Kt4 age (late Katian in Videt et al., 2010). In the present study, the *A. merga* biozone is assigned to the Kt4 time slice and directly overlies the *A. nigerica* biozone (late Katian; Fig. 2). In addition, *Desmochitina* cf. *juglandiformis* and *Hyalochitina hyalophrys* are first included at the base of the present biozone (Fig. 2, MG-20). To date, *D. juglandiformis* has been recorded from the Upper Sandbian-Katian in the Vitrival-Bruyére Formation and from the base of the Katian Fosses Formation in Belgium (Vanmeirhaeghe, 2006), from the Upper Ordovician in the Arabian Peninsula (Al-Hajri, 1995), and from Laurentia and the *B. robusta* biozone in northern Gondwana (southern Spain only; Vanmeirhaeghe, 2006). In Hartfell Score, Scotland (Laurentia), this species was recorded from the upper part of the graptolite *wilsoni* biozone to the lower part of the graptolite *clingani* biozone (Zalasiewicz et al., 2004), and from the Upper Ordovician in the British historical type areas and adjacent key sections (Vandenbroucke, 2008). *Hyalochitina hyalophrys* has been recorded from the late Ordovician, lower Ktaoua, and upper Tiouririne formations, Bou-Ingarf section, Central Anti-Atlas, Morocco (Bourahrouh et al., 2004).

Fig. 9. A, E. *Armoricochitina nigerica* (Bouché, 1965); B, F. *Armoricochitina iranica* Ghavidel-Syooki and Winchester-Seeto, 2002; C, G. *Armoricochitina persianense* n. sp.; D, H. *Armoricochitina persianense* n. sp.; I, M. *Spinachitina bulmani* Jansonius, 1964; J. *Armoricochitina nigerica* (Bouché, 1965); K, L. *Armoricochitina alborzensis* Ghavidel-Syooki and Winchester-Seeto, 2002; N. *Desmochitina* cf. *juglandiformis* Laufeld, 1967; O. *Desmochitina minor* Eisenack, 1931; P. *Desmochitina typica* Eisenack, 1931; Q. *Belonechitina wesenbergensis* (Eisenack, 1959); R, S, T. *Armoricochitina nigerica* (Bouché, 1965).

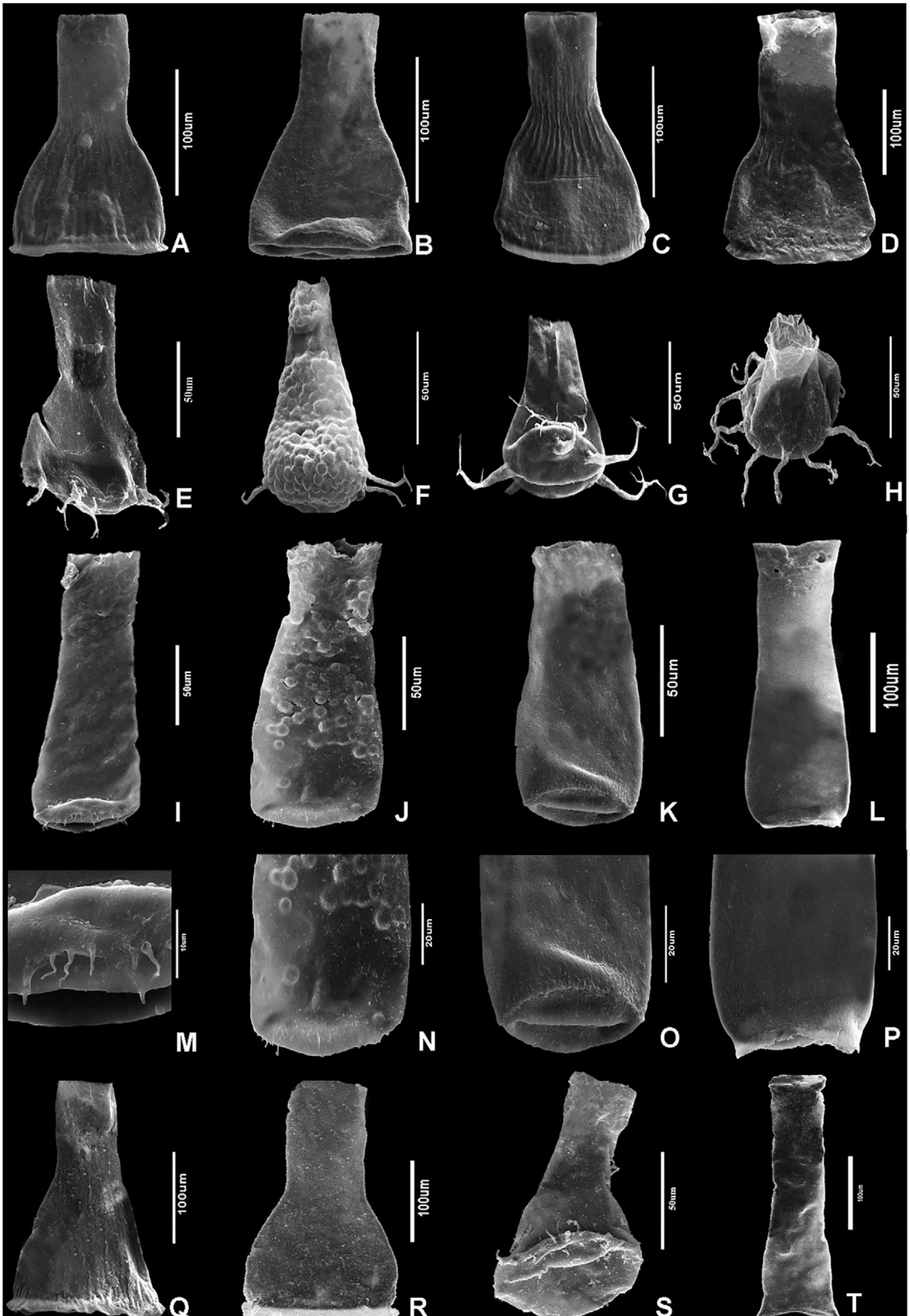
100um
A
100um
B
100um
C
100um
D
50um
E
50um
F
50um
G
50um
H
50um
I
50um
J
50um
K
100um
L
10um
M
20um
N
20um
O
20um
P
100um
Q
100um
R
50um
S
100um
T

3.1.5. Tanuchitina elongata biozone

In the present study, *Tanuchitina elongata* is considered a senior synonym of *Tanuchitina bergstromi* (see supplementary reference list S13, Laufeld, 1967). This biozone is marked by the FAD of *T. elongata* in sample MG-22C and extends throughout the lower unit of the Glacial Member of the Ghelli Formation (Fig. 2). It corresponds to the partial-range biozone of *T. elongata* (Bouché, 1965), from its first occurrence up to the FAD of *S. oulebsiri* (Webby et al., 2004), which is the index species of the succeeding biozone. *Tanuchitina elongata* biozone used to be the highest chitinozoan biozone in the North Gondwana Domain (Paris, 1990), but Paris et al. (2000a) found that the Upper Ordovician marine glacial sediments in Well NL-2 (northeastern Algerian Sahara) included a new chitinozoan species, *S. oulebsiri*, in the M' Kratta Formation, suggesting a late Hirnantian age. The *T. elongata* biozone is well documented in the North Gondwana Domain (Abuhmida, 2013; Al-Hajri, 1995; Bouché, 1965; Elaouad-Debbaj, 1984; Ghavidel-Syooki, 2008; Ghavidel-Syooki et al., 2011; Ghavidel-Syooki, 2016a, 2016b; Oulebsir and Paris, 1995; Paris, 1990; Paris et al., 2007, 2015). According to McClure (1988) and Paris (1990), at least the upper part of the Ra'an Shale Member of the Qasim Formation in the Arabian Peninsula is a *T. elongata* biozone, and this is associated with the *Glyptograptus persculptus* graptolite zone, suggesting it belongs to the Hirnantian stage (Webby et al., 2004). In addition, *P. comma*, *Tanuchitina alborzensis* n. sp., and *Conochitina rotundata* (Paris et al., 2015) have their first inception at the base of this biozone (MG-23C). *Pistillachitina comma* has been recorded from the Katian of the Baltic area (see supplementary reference list S13, Eisenack, 1959) and *C. rotundata* from the late Ordovician (Hirnantian) in the Quwarah Member of the Qasim Formation in the Arabian Peninsula (Paris et al., 2015). The *T. elongata* biozone is usually recorded in the North Gondwana Domain between the *A. merga* and *S. oulebsiri* biozones and thus attributed to the early Hirnantian (Hi1). The basal part of the Glacial Member of the Ghelli Formation also contains cephalopods, tentaculites, and crinoids (see Supplementary data, Fig. S5, D, G, H).

3.1.6. Spinachitina oulebsiri biozone

This chitinozoan biozone was recognized in the upper unit of the Glacial Member of the Ghelli Formation. The FAD of *S. oulebsiri* is observed in sample MG-41 and continues to sample MG-60 (Fig. 2). The *S. oulebsiri* biozone has been originally established in the Upper Member of the M' Kratta Formation, northeast Algerian Sahara, Bordj Nili area (Paris et al., 2000a), and was indirectly correlated with the *G. persculptus* graptolite zone of the late Hirnantian (Paris et al., 2000a; Webby et al., 2004). *Spinachitina oulebsiri* was recorded from the Hirnantian in numerous localities in North Africa (Abuhmida, 2013; Le Hérissé et al., 2013; Le Heron et al., 2008) and Iran (Ghavidel-Syooki, 2008; Ghavidel-Syooki et al., 2011; Ghavidel-Syooki, 2016a, 2016b). Accordingly, the *S. oulebsiri* biozone is of particular interest in the correlation of Late Ordovician strata and in the recognition of the Ordovician-Silurian boundary. Therefore, this chitinozoan biozone is used to define the upper part of Hi2 in the Ghelli Formation (Fig. 2). However, Butcher, 2009 (see supplementary reference list S13) has questioned the taxonomic validity of *S. oulebsiri*, and hence the usefulness of its biozone. This author demonstrated that it is impossible to find quantitative criteria to clearly distinguish *S. oulebsiri* from *S. fragilis* (Nestor, 1980) and that *S. oulebsiri* should be considered a junior synonym of *S. fragilis*. According to Paris et al. (2000a, p. 101), *S. oulebsiri* could be an early morphotype of the *S. fragilis* lineage characterized “by the increase of the vesicle's length, progressive differentiation of the flexure, and development of a crown of spines on the basal margin as well as on the oral pole margin. Vandenbroucke et al. (2009) also recognized, it is difficult to distinguish species within the *S. oulebsiri*–*S. fragilis* lineage, especially in moderately preserved material. However, this author decided to retain the two species separately until more detailed analyses are performed, the two morphotypes (conical vs. cylindrical basal spines and overall stouter vs. slender chamber in *S. oulebsiri* vs. *S. fragilis*, respectively).

In the present study, *S. oulebsiri* specimens were suitable for a taxonomical analysis and revision, because chitinozoan and acritarch taxa of the Ghelli and Niur formations indicating the Late Ordovician and Early Silurian were well preserved. Some diagnostic chitinozoan species of the preceding biozones, namely *A. nigerica*, *C. rotundata*, *D. typica*, and *P. comma*, were also present in the *S. oulebsiri* biozone, which is characterized by the co-occurrence of the chitinozoans *Tanuchitina anticostiensis*, *Belonechitina tenuicomata*, *Spinachitina iranense* n. sp., and *Cyathochitina caputoi*. Most acritarch taxa of the preceding biozones disappear at the onset of this chitinozoan biozone, and only two acritarch species, *Multiplicisphaeridium irregulare* and *Ordovicidium elegantulum*, continue within it (Fig. 2). *Belonechitina tenuicomata*, *T. anticostiensis*, and *C. caputoi* appear at the onset of the *S. oulebsiri* biozone and extend to the upper unit of the Glacial Member of the Ghelli Formation. These species were only recorded from the Late Ordovician (Canada, Libya, Arabian Peninsula, and Iran; Achab, 1978; Ghavidel-Syooki et al., 2011; Ghavidel-Syooki, 2016a, 2016b; Molyneux and Paris, 1985; Paris et al., 2015). This chitinozoan biozone is associated with thin–medium bedded pelmatozoan-bryozoan limestones (see Supplementary data, Fig. S6, E, F) containing abundant shelly fauna such as bryozoans (50%), brachiopods (25%), cystoids (7%), echinoderms (5%), tentaculites (2%), and very few trilobites (1%). These types of biostrome beds are recorded for the first time from the Hirnantian in Iran, whereas shallow-water carbonates of Ashgill age were recorded throughout the Northern Gondwana Domain during the periglacial episode in the Katian that preceded the latest Ordovician glacial event in the Hirnantian (Vennin et al., 1998). To date, carbonate deposits have been designated bryozoan biostromes in the subsurface of Djeffara Formation in Libya (see supplementary reference list S13, Bergström and Massa, 1991), Khant-el-Hajar bryozoan limestones in the Moroccan Anti-Atlas (Destombes et al., 1985), and Cystoid limestones in the Iberian Chains, NE Spain (Vennin et al., 1998). The trilobite *Dalmanitina* (*Dalmanitina*) *subandina* (Monaldi and Boso, 1987) is found in the lowermost part of the *S. oulebsiri* biozone of the Glacial Member of the Ghelli Formation (see Supplementary data, Fig. S7, A). This trilobite was previously recorded from the Zapla Formation, uppermost Ordovician (Hirnantian) in northwestern Argentina (Benedetto et al., 2015). It should also be mentioned that associated shelly fauna must be analyzed in detail considering facies, sedimentary environment, and sequence stratigraphy, to achieve a better understanding of the paleoecological patterns and paleogeographical constraints of these limestones in the Ashgill-aged Northern Gondwana Domain.

3.1.7. Spinachitina fragilis biozone

This biozone is marked by the FAD of *S. fragilis* in sample MG-60 and its continuation to sample MG-65 (Fig. 2) of the Niur Formation. From base to top, the Niur Formation comprises the Shale, Carbonate, and Sandstone Members. The chitinozoan fauna found in the Shale Member of the Niur Formation revealed that it is related to the latest Ordovician (Hirnantian), although the Carbonate and Sandstone members belong to the lower Silurian. Therefore, if we accept the old subdivision of the Niur Formation (Afshar-Harb, 1979), this formation is a diachronous rock unit, whereas if we use the new subdivisions of the Ghelli and Niur formations, these belong to the Ordovician and Silurian, respectively. The *S. fragilis* biozone corresponds to the total range of

Fig. 10. A, C, R. *Cyathochitina campanulaeformis* Eisenack, 1931; B. *Cyathochitina caputoi* Da Costa, 1971; D, Q. *Cyathochitina latipatagium* Jenkins, 1969; E. *Ancyrochitina bifurcaspina* Nestor, 1994; F, G, H. *Ancyrochitina merga* Jenkins, 1970; J, N. *Spinachitina bulmani* Jansonius, 1964; I, M. *Spinachitina fragilis* (Nestor, 1980); K, O. *Spinachitina* cf. *kourneidaensis* (Bouché, 1965); L, P. *Tanuchitina ontariensis* Jansonius, 1964; S. *Fungochitina actonica* (Jenkins, 1967); T. *Tanuchitina fistulosa* (Taugourdeau and de Jekhowskey, 1960).

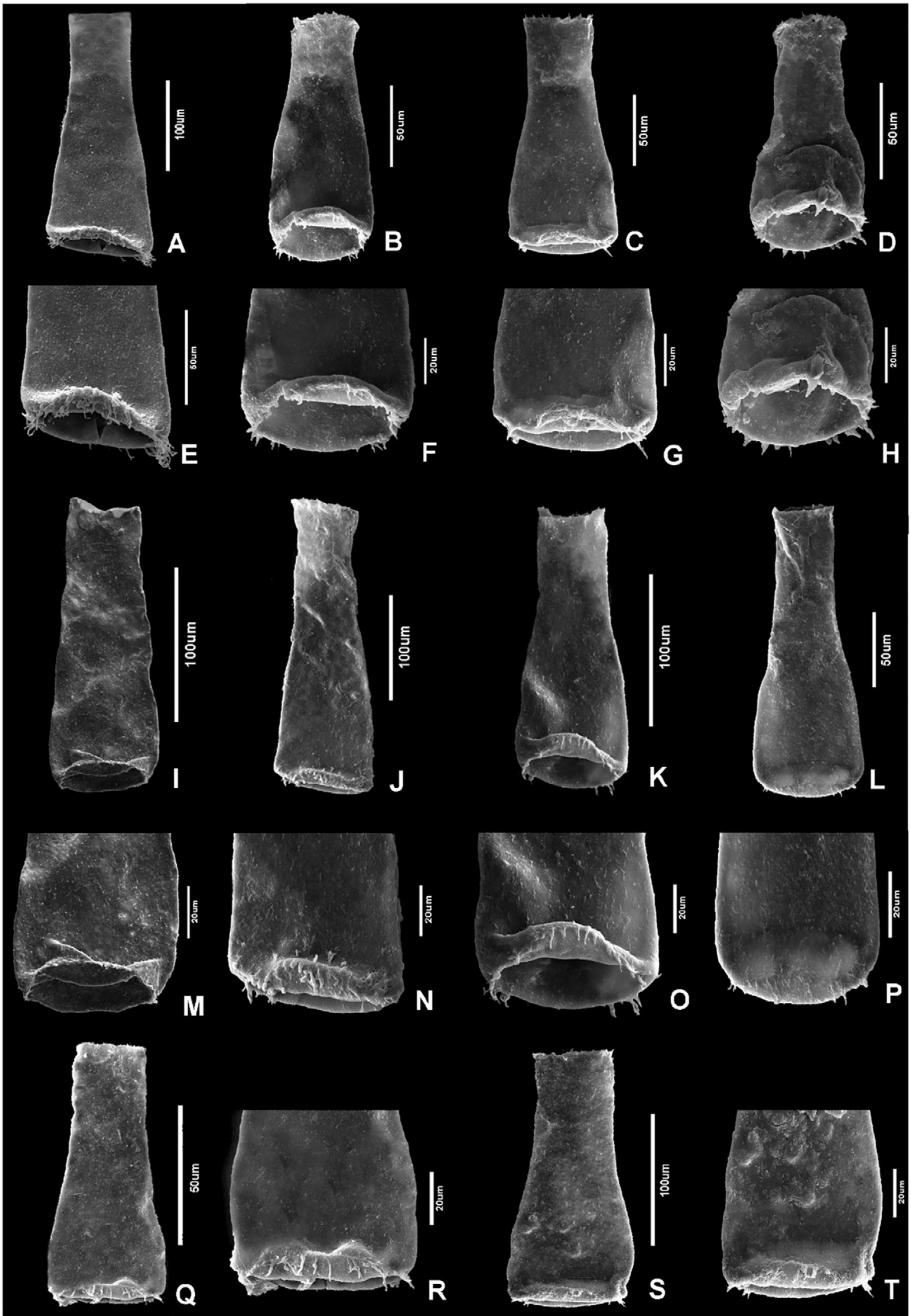
100um
A
50um
B
50um
C
50um
D
50um
E
20um
F
20um
G
20um
H
100um
I
100um
J
100um
K
50um
L
20um
M
20um
N
20um
O
20um
P
50um
Q
20um
R
100um
S
20um
T

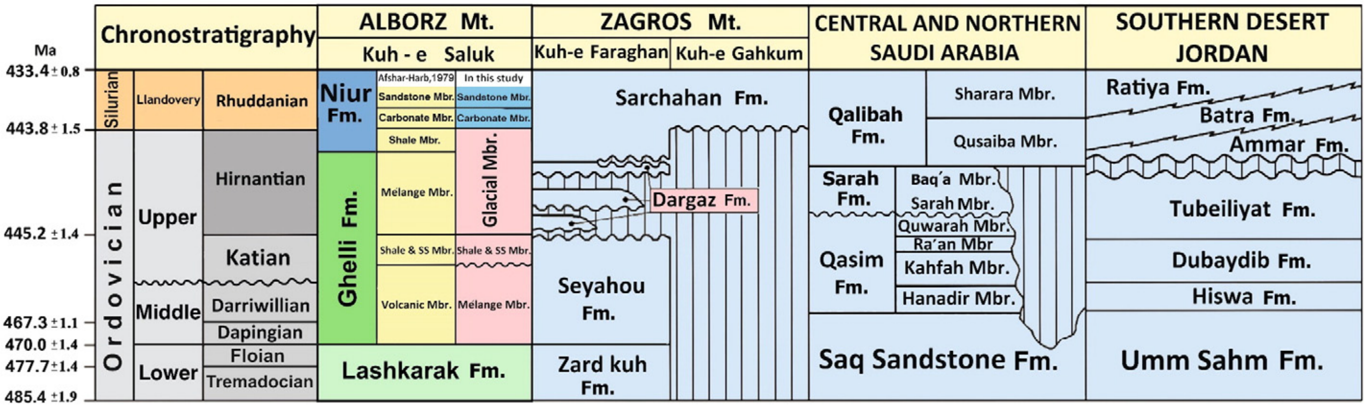

Fig. 12. Summarized chronographic and lithostratigraphic chart of the Zagros Mountains, Alborz Mountains, Saudi Arabia, and Jordan, based on Vaslet (1990), Armstrong et al. (2005), Clark-Lowes (2005), Turner et al. (2005), Ghavidel-Syooki et al. (2011), Melvin (2015), Paris et al. (2015), Cohen et al. (2016), Ghavidel-Syooki (2016a, 2016b), and the present work.

Ancyrochitina laevaensis (Nestor, 1980) biozone in the lowermost Llandovery (Rhuddanian). To date, *S. fragilis* was recorded from the early Llandovery strata in Estonia (Nestor, 1980) and north Latvia (Nestor, 1994). Verniers et al. (1995) designated the *S. fragilis* biozone as the lowermost global Silurian chitinozoan biozone. *Spinachitina fragilis* has been recorded from the lower Llandovery (Rhuddanian) in the Arabian Peninsula (Paris et al., 1995); the early Llandovery *ascensus–acuminatus* graptolite zones in Jordan (Butcher, 2009); the *Normalograptus persculptus* biozone (Hirnantian) in the lower part of the Sarchahan Formation in Zagros Mountains, southern Iran (Ghavidel-Syooki and Winchester-Seeto, 2004; Ghavidel-Syooki et al., 2011); and lower Silurian, in the lower part of the Tanezzuft Formation, Well B2-NC 186 in Libya (Abuhmida, 2013). Other chitinozoan species occurring exclusively in the *S. fragilis* biozone are *Ancyrochitina bifurcaspina* and *Plectochitina nodifera*. These two species also occur in the early Llandovery strata from Baltica and northern Gondwana (Nestor, 1980, 1994; Vernier et al., 1995). In the present study, *S. fragilis* and *S. oulebsiri* were retained as two separate species due to their differences in morphology, associated taxa, and FAD (Fig. 2; Supplementary data, S3).

3.2. Acritarch biostratigraphy

The acritarch assemblage found in the type section of the Ghelli Formation comprises 18 species (10 genera). These allowed recognizing the two local acritarch assemblage zones (Fig. 2), which are discussed below in ascending stratigraphic order.

3.2.1. Acritarch assemblage zone I

This biozone is characterized by the occurrence of several acritarch taxa between samples MG-08 and MG-22C, along the 412 m of the Shale and Sandstone Member of the Ghelli Formation. This biozone is well defined by the appearance of Upper Ordovician acritarch taxa including: *Acanthodiacrodium crassus* (Loeblich and Tappan, 1978) Vecoli, 1999; *Villosacapsula setosapellicula* (Loeblich) Loeblich and Tappan, 1976 (see supplementary reference list S13); *Multiplicisphaeridium irregulare* (Staplin et al., 1965); *Multiplicisphaeridium bifurcatum* (Staplin et al., 1965); *Orthosphaeridium insculptum* (Loeblich, 1970); *Orthosphaeridium bispinosum* (see supplementary reference list S13, Turner, 1984); *Orthosphaeridium quadrinatum* (see supplementary reference list S13, Burmann, 1970) Eisenack et al., 1976; *Ordovicidium elegantulum* (see supplementary reference list S13, Loeblich and Tappan, 1970); *Dactylofusa cabottii* (Cramer) Fensome et al., 1990; *Baltisphaeridium oligopsakium* (Loeblich and Tappan, 1978); *Baltisphaeridium perclarum* (Loeblich and Tappan, 1978); *Dorsennidium hamii* (Loeblich) Sarjeant and Stancliffe, 1994, see supplementary reference list S13; *Diexapllophasis denticulata* (Stockmans and Williére) Loeblich, 1970; *Neoveryhachium* sp. cf. *carminae* (Cramer) Cramer, 1971, see supplementary reference list S13, *Veryhachium lairdii* (Deflandre) Deunff, 1959 ex Downie, 1959; see supplementary reference list S13, *Navifusa ancepsipuncta* (Loeblich, 1970 ex Eisenack et al. 1979); *Leiofusa litotes* (Loeblich and Tappan, 1978); *Muzivum gradzinskii* (Wood and Turnau, 2001; *Veryhachium inflatum* (see supplementary reference list S13, Hashemi and Playford, 1998).

Villosacapsula setosapellicula has been recorded from the Richmondian (Katian) of Oklahoma (Loeblich, 1970) and Missouri (Wicander et al.,1999), the Katian of Algerian Sahara (see supplementary reference list S13, Jardine et al., 1972), Libya (Molyneux and Paris, 1985; see supplementary reference list S13, Hill and Molyneux, 1988), Canada (Jacobson and Achab, 1985), Jordan (see supplementary reference list S13, Keegan et al., 1990), the Arabian Peninsula (Le Hérissé et al., 2015), and Iran (Ghavidel-Syooki, 2008; Ghavidel-Syooki et al., 2011; Ghavidel-Syooki, 2016a, 2016b), and the Upper Ordovician (Katian) of Morocco (see supplementary reference list S13, Elaouad-Debbaj, 1988). Similarly, *B. perclarum* has been recorded from the Richmondian (Katian) of Oklahoma (Loeblich and Tappan, 1978) and Missouri (Wicander et al., 1999), the Ashgillian (Katian) strata of Canada (Jacobson and Achab, 1985) and Iran (Ghavidel-Syooki, 2008; Ghavidel-Syooki et al., 2011; Ghavidel-Syooki, 2016a, 2016b), the Upper Ordovician (Katian) of Jordan (Keegan et al., 1990), and the Katian of the Arabian Peninsula (see supplementary reference list S13, Jachowicz, 1995; Le Hérissé et al., 2015). *Orthosphaeridium insculptum* has been recorded from the Sylvan Shale (Katian) of Oklahoma (Loeblich, 1970), the Maquoketa Shale (Katian) of northeastern Missouri (Wicander et al., 1999), the Vaureal Formation (Katian) of the Anticosti Island, Québec, Canada (Jacobson and Achab, 1985), the Upper Ordovician (Katian) of Czech Republic (Vavrdová, 1989), and the Ashgill deposits of Portugal (see supplementary reference list S13, Elaouad-Debbaj, 1981) and Morocco (Elaouad-Debbaj, 1988). It was also reported from the Upper Ordovician (Katian) Seyahou Formation of the Zagros Mountains, southern Iran (Ghavidel-Syooki et al., 2011), and from the Ghelli Formation, northeastern Alborz Mountains (Ghavidel-Syooki, 2000; Ghavidel-Syooki et al., 2011; Ghavidel-Syooki, 2016a, 2016b). *Acanthodiacrodium crassus* has been

Fig. 11. A, E. *Spinachitina iranense* n. sp.; B, F. *Spinachitina oulebsiri* Paris et al., 2000a; C, G. *Spinachitina oulebsiri* Paris et al., 2000a; D, H. *Spinachitina oulebsiri* Paris et al., 2000a; I, M. *Spinachitina fragilis* (Nestor, 1980); J, N. *Spinachitina oulebsiri* Paris et al., 2000a; K, O. *Spinachitina oulebsiri* Paris et al., 2000a; L, P. *Spinachitina oulebsiri* Paris et al., 2000a; Q, R. *Spinachitina oulebsiri* Paris et al., 2000a; S, T. *Spinachitina oulebsiri* Paris et al., 2000a.

recorded from the Upper Ordovician (Katian) of Czech Republic (supplementary reference list S13, Vavrdová, 1989), North America (Jacobson and Achab, 1985; Wicander et al., 1999), and Portugal (Elaouad-Debbaj, 1981), and the Katian of North Africa (Elaouad-Debbaj, 1988; see supplementary reference list S13, Vecoli, 1999), Arabian Peninsula (Le Hérissé et al., 2015), and Iran (Ghavidel-Syooki, 2008; Ghavidel-Syooki et al., 2011).

Baltisphaeridium perclarum, *N. ancepsipuncta*, *B. oligopsakium*, *O. insculptum*, and *A. crassus* are critical acritarch taxa, which are restricted to the Katian. Furthermore, acritarch taxa such as *O. octospinosum*, *O. bispinosum*, *M. irregulare*, *M. bifurcatum*, *O. elegantulum*, *V. lairdii* group, and *O. quadrinatum* are found in the Middle to Upper Ordovician strata of Sweden (see supplementary reference list S13, Górka, 1987; Kjellström, 1971), United States (see supplementary reference list, S13, Colbath, 1979; Loeblich and Tappan, 1978), Czech Republic (see supplementary reference list S13, Vavrdová, 1989), Arabian Peninsula (see supplementary reference list S13, Jachowicz, 1995; Le Hérissé et al., 2013, 2015), China (Li et al., 2006), and Iran (Ghavidel-Syooki, 2000, 2008; Ghavidel-Syooki et al., 2011; Ghavidel-Syooki, 2016a, 2016b). Based on the acritarch biostratigraphy of the *Dicellogratus complanatus* graptolite zone from the Katian Vaureal Formation of Anticosti Island, Québec, Canada (Jacobson and Achab, 1985) and on the Katian Maquoketa Shale of northeastern Missouri (Wicander et al., 1999), the acritarch taxa found in this assemblage zone suggest that the Shale and Sandstone Member of Ghelli Formation belongs to the Upper Ordovician (Katian). This is consistent with standard Ordovician chitinozoan biozonations (Paris, 1990, 1996).

3.2.2. Acritarch assemblage zone II

This biozone is marked by the occurrence of several acritarch taxa between samples MG-22C and MG-64, across the 404 m of the Glacial Member of the Ghelli Formation (Fig. 2). This assemblage is well defined by the appearance of Upper Ordovician (Hirnantian) acritarch taxa, namely *Inflatarium trilobatum* (Le Hérissé et al., 2013), *Safirotheca safira* (Vavrdová, 1989), *Dactylofusa striatifera* (Cramer and Diez) Fensome et al., 1990, *Dactylofusa cabottii* (Cramer) Fensome et al., 1990, *Muzivum gradzinskii* (Wood and Turnau, 2001), and *Neoveryhachium* sp. cf. *carminae* (Cramer) Cramer, 1971. *Inflatarium trilobatum* has only been recorded from the Late Ordovician (late Katian–early Hirnantian) in the Quwarah Member of the Qasim Formation in the Arabian Peninsula (Le Hérissé et al., 2013, 2015). In the present study, this species occurs in the entire Glacial Member of the Ghelli Formation. To date, *S. safira* has been reported from the Upper Ordovician of the Czech Republic (Vavrdová, 1989), the Hirnantian glacial deposits of the Zagros Mountains (Dargaz Formation, Ghavidel-Syooki et al., 2011), the Mélange Member (equivalent to part of the Glacial Member in this study) of Ghelli Formation (Ghavidel-Syooki et al., 2011; Ghavidel-Syooki, 2016a, 2016b), and the Hirnantian glacial deposits of the Arabian Peninsula (Le Hérissé et al., 2015). *Neoveryhachium* sp. cf. *carminae*, appears in samples MG-23 to MG-64 of the Ghelli Formation (Fig. 2), marking the beginning of the *S. oulebsiri* biozone. It is worth mentioning that *D. cabottii* is a common palynomorph in Ordovician–Silurian shallow-water, near-shore marine strata (Gray and Boucot, 1989; Raevskaya and Dronov, 2014). It has also been reported from various non-marine deposits, and attributed to a possible old-euglenoid freshwater protozoan (Wood and Turnau, 2001). Because *D. cabottii* is widely distributed from near-shore to shelf marine strata, it can be considered with marine affinity until further evidence is obtained. *Muzivum gradzinskii* is another common palynomorph in the Glacial Member of the Ghelli Formation. This species has been recorded from the Devonian, in the Holy Cross Mountain and Radom–Lublin region of Poland, and assigned to family Hydrodictyaceae within the Chlorophyta. Based on its coenobial habit and on comparisons with extant Hydrodictyaceae, which are only found in fresh to brackish waters, the depositional environment of *M. gradzinskii* is interpreted as very near-shore to shelf marine strata. Some acritarch taxa of this assemblage zone, such as *S. safira*, *D. striatifera*, *I. trilobatum*, and *Neoveryhachium* sp., are restricted to the peri-Gondwana paleoprovince and represent the Hirnantian age (Le Hérissé et al., 2015; Vecoli and Le Hérissé, 2004). This is consistent with standard Ordovician chitinozoan biozonations (Paris, 1990, 1996).

4. Hirnantian stratigraphy and its paleogeographic implications

The glacial deposits of the Ghelli Formation are well differentiated from underlying (Shale and Sandstone Member of the Ghelli Formation) and overlying (Carbonate and Sandstone members of the Niur Formation) rock units (Fig. 2). The Shale and Sandstone Member of the Ghelli Formation is represented by ichnofossils such as *Cruziana*, *Rusophycus*, *Lockeia*, *Bifungites*, *Chondrites*, *Planolites*, *Bifasciculus*, *Monomorphichnus*, *Isopodichnus*, *Cochlichnus*, *Trichichnus*, and *Muensterria*, which are associated with rhythmic bedded tidalites of claystone and sandstone. The Glacial Member of the Ghelli Formation is characterized by three key events. The first is a transgressive-regressive cycle, which is marked by glaciogenic shoal deposits resting on a pre-glacial (Katian) substrate with a sharp erosive surface and incision (Fig. 3, C, D). The second is also related to a transgressive-regressive cycle, but it is bounded by two erosive surfaces at the base and top (Figs. 2 and 4, E, F). The third event mimics the previous one and is characterized by diamictites (pebbly mudstone) at the base (Figs. 3, A and 4, H), changing into black shale interbedded with biostrome beds upward the Glacial Member (Fig. 2; see Supplementary data, Fig. S6, E, F). Another subdivision is also possible based on the major erosive boundaries between sedimentary sequences. In this case, the Glacial Member, which extends from the upper part of the Shale and Sandstone Member of the Ghelli Formation to the Carbonate Member of the Niur Formation, is subdivided into transgressive-regressive cycles, including GES1, GES2, and GES3 (Fig. 2).

Paleocurrent measurements from the incisions recorded in the Glacial Member of the Ghelli Formation indicate a predominant north–northeast dipping paleoslope. This is in agreement with the orientation of the tunnel channels preserved in the Arabian Peninsula and Jordan (Clark-Lowes, 2005; Vaslet, 1990), suggesting there is a Hirnantian ice cap in the northeastern Alborz Mountains as well as in the Zagros Mountains close to the Arabian Plate. The magnitude of sea-level fluctuations associated with the Hirnantian glaciation could not be measured in the study area owing to insufficient sedimentological data. However, neighboring Hirnantian meltwater produced tunnel channel incisions ca. 4–6 km wide, 30–50 km long, and 100 m deep in the Arabian Peninsula (Clark-Lowes, 2005; Vaslet, 1990), Jordan (Powell et al., 1994; Turner et al., 2005), Libya (see supplementary reference list S13, Le Heron et al., 2004), Tassili N'Ajjer and In Amenas field in Illizi Basin, Algeria (Hirst et al., 2002; Hirst, 2015), and Anti-Atlas of Morocco (Le Heron et al., 2007, 2008). Incisions less than 40 m deep were produced in the Zagros Mountains (Ghavidel-Syooki et al., 2011).

Shelly fauna, such as tentaculites, cephalopods, trilobites, and echinoderms were recorded from pre-glacial siliciclastic sediments in the Seyahou Formation and from the *A. nigerica* biozone (Katian) in the Zagros Mountains, southern Iran, suggesting a Boda warming event (Fortey and Cocks, 2013; Ghavidel-Syooki et al., 2015). In the western part of Kuh-e Saluk, NE Alborz Mountains, the shelly fauna (echinoderms, bryozoans, cephalopods, trilobites, crinoids, and tentaculites) is distributed in two distinctive horizons of the Glacial Member. The first horizon, in the lower unit of the Glacial Member (see Supplementary data, Fig. S5, D, G, H) includes the uppermost parts of the *A. merga* and *T. elongata* biozones, which are assigned to the latest Katian–earliest Hirnantian (Kt4–Hi1); the second horizon occurs in the *S. oulebsiri* biozone, which is related to the upper Hirnantian (Hi2).

The upper unit of the Glacial Member is characterized by the alternation of black papery shale with thin–medium biostrome beds containing common echinoderms (*Caryocrinites* sp., *Heliocrinites* sp., and *Hemicosmites* sp.; see Supplementary data, Fig. S6, A, C, and Fig. S7, C), abundant brachiopods (see Supplementary data, Fig. S6, A, C), extremely abundant bryozoans (Fig. 5, F, G, J; see Supplementary data, Fig. S7, B, D, F, G, H), rare tentaculites (see Supplementary data, Fig. S7, B), rare cephalopods (see Supplementary data, Fig. S7, E), and very rare trilobites (see Supplementary data, Fig. S7, A). Clastic deposition is universal and predominant during the Ordovician in high-latitude Gondwana regions, including North Africa, the Arabian Peninsula, the Iberian Peninsula, Sardinia, Armorica, and terranes marginal to the supercontinent northward the Saxo-Thuringian terrane. Deposition in this large area is considered to occur under shallow but cold water regimes. However, thick clastic sequences are interrupted in the Ashgillian by the appearance of limestone formations of Cautleyan–Rawtheyan age. Some authors (Boucot et al., 2003; Vennin et al., 1998; Villas et al., 2002) reported these limestones through several terrains in Spain and elsewhere, the classical development being the Cystoid Limestone of the Iberian Chains. Contemporary limestones extend into Sardinia (upper part of the Domunovas Formation), Armorica (Porzhig Member), Montagne Noire in France, Carnic Alps (Uggwa Limestone), and Libya (upper Djeffara Formation). The abrupt appearance of these limestones contrasts with the thick clastic sequences below and above. In the studied area, coquina, or biostrome beds, are recorded for the first time from the latest Ordovician (Hirnantian) in the Iranian Platform. To date, the high-latitude carbonate deposition over the Gondwana landmass has been assigned to late Katian (Fortey and Cocks, 2013), not Hirnantian. Boucot et al. (2003) suggested a climatic warming in the Mediterranean region at this time, which was designated by Fortey and Cocks (2013) as the Boda warming event. According to the chitinozoan biostratigraphic charts published by Paris (1990) and Videt et al. (2010), and to comparisons with the chitinozoan biozones of the Ghelli Formation, the shelly fauna of the Glacial Member of this formation are assigned to the Hirnantian. Therefore, the coquina or biostrome beds in the Glacial Member of this formation are not related to the Katian Boda warming event. Although the interpretation of the coquina or biostrome beds of the Glacial Member of this formation in the Hirnantian interval is difficult, they might have resulted from climatic amelioration rather than local reduction of clastic input. Lithological changes are likely due to a short global warming episode during the Hirnantian interval. Similar to the chitinozoan biozones of the Ghelli Formation, all shelly fauna of the Glacial Member must be studied by several specialists to clarify their relationships with climatic amelioration and variations in oceanic circulations. Stratigraphic correlation among the very different sequences of the late Ordovician is difficult, and further work is therefore necessary to establish the synchronicity of the various proposed events.

5. The Iranian Platform fringing the Arabian margin of Gondwana

The Arabian Plate is a tectonostratigraphic term widely used in early Paleozoic paleogeographic reconstructions, the "plate" came into existence only in the Oligocene (Melvin et al., 2003; Moscariello et al., 2008; Vaslet, 1989, see supplementary reference list S13; Vaslet, 1990). Since then, the rocks that comprise what is now the Arabian Peninsula, Syria, Jordan, Iraq, and Iran (including Zagros and Alborz Mountain Ranges and Central Iran) began to separate from the African continent due to the rifting along the margin of northeast Africa, and to the opening of the Red Sea and the Gulf of Aden (Ghavidel-Syooki et al., 2011, Fig. 1A). Thus, throughout the Neoproterozoic to the end of the Paleozoic, the Arabian Plate was part of Gondwana. During the Neoproterozoic, the Iranian Platform was located near the Equator but in the Cambrian–Ordovician it followed the southward drift that characterized West and East Gondwana, reaching ca. 60° S latitude during the Silurian (Ghavidel-Syooki and Vecoli, 2007; Heydari, 2008; Torsvik and Cocks, 2009). On the Arabian margin, Hirnantian glaciogenic rocks and tunnel valleys have been reported in the Al Qasim district, in the Wajid and Widyan plateau of the Arabian Peninsula (Clark-Lowes, 2005; Dabard et al., 2015; McClure, 1978; Melvin, 2015; Vaslet, 1990), and in the southern desert of Jordan (Armstrong et al., 2009; Turner et al., 2005). The position of these tunnel valleys and the glacially scoured paleoreliefs at the surface and subsurface of the Arabian Peninsula suggest that the glaciated source area was located across the Arabian–Nubian Shields, and that sediments were transported along the present-day east to northeast direction (Ghavidel-Syooki et al., 2011; Le Heron and Dowdeswell, 2009). The northwest of the Arabian Peninsula formed part of a more extensive ice sheet, similar in size to that of the current Antarctic ice sheet (Le Heron and Dowdeswell, 2009).

Current models for the Hirnantian glaciation in Jordan recognized two major glaciation phases (Abed et al., 1993), which are correlatable with the two major glacial advances and retreats recorded in the northwest of the Arabian Peninsula (Al-Harbi and Khan, 2011; Vaslet, 1990). However, Turner et al. (2005) proposed a four-stage glacial model where the ice preferentially excavated fault-controlled depressions (reactivation of faults might be related to hydrothermal activity), cutting steep-sided U-shaped valleys. The fourth glacial stage of Jordan would be coeval to the second glacial phase of the Arabian Peninsula, which was reinterpreted by Miller and Mansour (2007) and, more recently, by Melvin (2015). In this study, the authors described a more complex record of ice advance and retreat in the Sarah Formation. Similarly, two major Hirnantian sequences are recognized in Spain (Álvaro and Van Vliet-Lanoë, 2009), Morocco (Loi et al., 2010), Mauritania (Ghienne, 2003), and Turkey (Monod et al., 2003), although in the last two regions each major sequence has been subsequently subdivided into two higher frequency cycles. These cycles have not been widely recorded, but the patterns of major ice advances interrupted by smaller-scale pulses have been interpreted as reflecting eccentricity and obliquity moderated ice volume changes (Armstrong et al., 2009; Sutcliffe et al., 2000).

In NE Alborz Mountains, the Glacial Member of the Ghelli Formation comprises three progradational-retrogradational cycles, each potentially controlled by the regional advance and retreat of the Hirnantian ice sheet. In the study area, the glacial deposits of the Ghelli Formation are overlain by the Niur Formation, which consists of Carbonate and Sandstone Members. Based on its stratigraphic position, the Shale Member of the Niur Formation was previously assigned to early Silurian (Afshar-Harb, 1979), but the present study revealed that it belongs to the latest Hirnantian. This new age assignment is based on the presence of diagnostic chitinozoan and acritarch species such as *S. oulebsiri*, *A. nigerica*, *C. rotundata*, *P. comma*, *E. moussegoudaensis*, *N. ancepsipuncta*, *A. crassus*, and *V. setosapellicula* (Fig. 2). In the Pelmis Gorge and in Ghelli village, located in the eastern and western parts of Kuh-e Saluk in Alborz Mountains, respectively, the transition from the Ghelli to the Niur Formation is similar to that of the Seyahou to Sarchahan Formation in the Zagros Mountains (kerogenous rocks with reducing condition; Ghavidel-Syooki et al., 2011; Ghavidel-Syooki, 2016a).

The abrupt end of the Hirnantian glaciation is marked by extensive marine flooding that deposited organic-rich hot shales across large areas of the Arabian Plate and North Africa. The final stage of glaciation provided the ideal conditions for deposition of kerogenous rocks. The reducing conditions at the seafloor were sufficient to produce and preserve organic matter rich in radioactive elements responsible for the distinctive ‘hot response’ of gamma ray logs. In Iran, Ordovician to Silurian transition deposits are a proven source of hydrocarbons throughout North Gondwana, from Morocco to the Zagros and Alborz Mountains (Bordenave, 2008; Ghavidel-Syooki et al., 2011; Ghavidel-Syooki, 2016a). Thus, the glacial events affected the African-Arabian margin of Gondwana and had a major impact on the petroleum and gas systems in this region, resulting in the deposition of source rocks immediately after the final glaciation (Bell and Spaak, 2006). In addition, in the Lut Block of Central Iran, the Ordovician to Silurian transition is associated with transtensive extension and syn-rift volcanism. These phenomena led to the deposition of flood basalts up to 500 m thick over the 1000 km that neighbor the Arabian margin and were an integral part of Gondwana during the Ordovician (Bagheri and Stampfli, 2008; Berberian and King, 1981; Husseini, 1990; Torsvik and Cocks, 2009).

6. Conclusions

Hirnantian glacial deposits are exposed in the western part of Kuh-e Saluk, in the type locality of the Ghelli Formation in NE Alborz Mountains. In the stratotype area of this formation, glaciogenic deposits consist of gray sandstone in the upper part (40 m) of the Shale and Sandstone and Mélange members (224 m) of the Ghelli Formation, and Shale Member (140 m) of the Niur Formation. These were grouped into a new lithostratigraphic "Glacial Member", which is more than 400 m thick and is recorded for the first time from the NE Alborz Mountains, Iran. The Glacial Member comprises three progradational-retrogradational sedimentary cycles (bounded by three glacial erosive surfaces), each potentially controlled by the regional advance and retreat of the Hirnantian ice sheet. The glaciated source area was located west of the study area, in the Arabian Shield, a region characterized by numerous tunnel valleys. Based on well-known chitinozoan biozones, the Glacial Member of the Ghelli Formation is attributed to the Hirnantian age, whereas the Niur Formation is assigned to the early Silurian (Rhuddanian). The abrupt end of the Hirnantian glaciation is marked by an extensive marine flooding that deposited organic-rich kerogenous shales across large areas of the Arabian Peninsula and North Africa.

The Ordovician–Silurian transition deposits are hydrocarbon sources throughout North Gondwana, from Morocco to the Zagros and Alborz Mountains in Iran. Therefore, the glacial events that affected the African-Arabian margin of Gondwana had a major impact on the petroleum and gas systems of this region and resulted in the deposition of source rocks, immediately after the final glaciation. In NE Alborz Mountains, the biostrome beds bearing echinoderms, crinoids, bryozoans, cephalopods, trilobites, and tentaculites are distributed in two distinctive horizons within the glacial deposits of the Ghelli Formation. The first fossiliferous horizon occurs in the lower unit of the Glacial Member, includes the *T. elongata* biozone, and is attributed to the Hi1 time slice. The second horizon occurs in the upper unit of the Glacial Member, includes the *S. oulebsiri* biozone, and is assigned to the Hi2 time slice. The high-latitude carbonate deposition recorded over the Gondwana landmass, embracing North Africa, the Iberian Peninsula, Sardinia, Armorica, and terranes marginal to the supercontinent northward to the Saxo-Thuringian terrane, are attributed to the Boda warming event in the late Katian. The biostrome beds of the Glacial Member of the Ghelli Formation are restricted to the Hirnantian interval and, therefore, are not related to the Boda event. Currently, the interpretation of the coquina or biostrome beds of the Glacial Member of the Ghelli Formation in the Hirnantian interval is difficult, but this carbonate deposit event might be the result of climatic amelioration rather than local reduction of clastic input. Observed lithological changes are likely explained by a short-lived episode of global warming during the Hirnantian interval.

Finally, our findings suggest the presence of a Hirnantian ice cap in the Alborz Mountains adjacent to Arabian Plate and allow filling a knowledge gap concerning the peripheral extension of the Late Ordovician ice sheet.

Acknowledgments

The author wishes to thank Prof. Florentin Paris, Mr. Saeed Al Tofaif, and an anonymous reviewer for their helpful comments and suggestions to improve this manuscript. Likewise, the author would like to thank Mrs. Zahra Orak for the palynological analysis of samples, and Dr. E. Mortezazadeh, Dr. M. Yousefi, and Mr. M. H. Piri for drawing tables and figures. The author specially thanks his wife and his daughter, Hedieh Ghavidel-Syooki, for their encouragement to finalize this contribution.

Appendix A. Supplementary data

Supplementary data associated with this article can be found in the online version, at http://dx.doi.org/10.1016/j.palaeo.2017.08.004. These data include the Google maps of the most important areas describe in this article.

References

Abed, M.B., Makhlouf, I.M., Amireh, B.S., Khalil, B., 1993. Upper Ordovician glacial deposits in southern Jordan. Episodes 16, 316–328.
Abuhmida, F., 2013. Palynological Analysis of the Ordovician to Lower Silurian Sediments From the Murzuq Basin, Southwest Libya. (Ph. D thesis). 64. University of Sheffield Department of Animal and Plant Sciences.
Achab, A., 1978. Sur Quelques Chitinozoaires de la Formation de Vauréal et de la Formation Macasty (Ordovicien Supérieur); Ile d' Anticosti, Québec, Canada. Rev. Palaeobot. Palynol. 25 (3–4), 295–314.
Afshar-Harb, A., 1979. The Stratigraphy, Tectonic and Petroleum Geology of Kopet Dagh Region. (Unpublished Ph. D. thesis). 316. Imperial College of Sciences and Technology, University of London.
Al-Harbi, O.A., Khan, M., 2011. Source and origin of glacial paleovalley-fill sediments (Upper Ordovician) of Sarah Formation in central Saudi Arabia. Arab. J. Geosci. 4 (5):825–835. http://dx.doi.org/10.1007/s12517-009-0097-2.
Álvaro, J.J., Van Vliet-Lanoë, B., 2009. Late Ordovician carbonate productivity and glaciomarine record under quiescent and active extensional tectonics in NE Spain. In: Bassett, M.G. (Ed.), Early Palaeozoic Peri-Gondwana Terranes: New Insights From Tectonics and Biogeography. 325. Geol. Soc., London, Spec. Publ., pp. 117–139.
Armstrong, H.A., Turner, B.R., Makhlouf, I.M., Weedon, G.P., Williams, M., Al Smadi, A., Abu Salah, A., 2005. Origin, sequence stratigraphy and depositional environment of an upper Ordovician (Hirnantian) deglacial black shale, Jordan. Palaeogeogr. Palaeoclimat. Palaeoecol. 220, 273–289.
Armstrong, H.A., Abbot, G.D., Turner, B.R., Makhlouf, I.M., Bayawa, M.A., Pedentchouk, N., Peters, H., 2009. Black shale deposition in an Upper Ordovician–Silurian permanently stratified peri-glacial basin, southern Jordan. Palaeogeogr. Palaeoclimatol. Palaeoecol. 273, 368–377.
Bagheri, S., Stampfli, G.M., 2008. The Anarak, Jandaq and Posht-e-Badam metamorphic complexes in central Iran: new geological data, relationships and tectonic implications. Tectonophysics 451, 123–145.
Bell, A., Spaak, P., 2006. Gondwana Glacial Events and Their Influence in the Petroleum System in Arabia. AAPG International Conference and Exhibition, Perth, Australia.
Benedetto, J.L., Halpern, K., de la Puente, G.S., Monaldi, C.R., 2015. An in situ shelly fauna from the lower Paleozoic Zapla diamictite of northwestern Argentina: implications for the age of glacial events across Gondwana. J. S. Am. Earth Sci. 64, 166–182.
Berberian, M., King, G.C., 1981. Towards a paleogeography and tectonic evolution of Iran. Can. J. Earth Sci. 18, 210–265.
Bordenave, M.L., 2008. The origin of Permo-Triassic gas accumulations in the Iranian Zagros foldbelt and contiguous areas: a review of Palaeozoic petroleum systems. J. Pet. Geol. 31, 3–42.
Boucot, A.J., Rong, J.-Y., Chen, X., Scotese, C.R., 2003. Pre-Hirnantian Ashgill climatically warm event in the Mediterranean region. Lethaia 36, 119–132.
Bourahrouh, A., Paris, F., Elaouad-Debbaj, Z., 2004. Biostratigraphy, biodiversity and palaeoenvironment of the chitinozoans and associated palynomorphs from the Upper Ordovician of the Central Anti-Atlas, Morocco. Rev. Palaeobot. Palynol. 130, 17–40.
Butcher, A., 2009. Early Llandovery chitinozoans from Jordan. Palaeontology 52, 593–629.
Carls, P., 1975. The Ordovician of the Eastern Iberian Chains near Fombuena and Luesma (Prov. Zaragoza, Spain). Neues Jb. Geol. Paläontol. Abh. 150, 127–146.
Chauvel, J., Le Menn, J., 1979. Sur quelques èchinodermes (cystoides et crinoides) de l'Asghill d'Aragon (Espagne). Geobios 12, 549–587.
Chauvel, J., Meléndez, B., Le Menn, J., 1975. Les Echinodermes (cystoides et crinoides) de l'Ordovicien supérieur de Luesma (Sud de l'Aragon, Espagne). Estud. Geol. 31, 351–364.
Cherns, L., Wheeley, J., 2009. Early Palaeozoic cooling events: Peri-Gondwana and beyond. Geol. Soc. Lond. Spec. Publ. 325 (1), 257–278.
Clark-Lowes, D.D., 2005. Arabian glacial deposits: recognition of palaeovalleys within the Upper Ordovician Sarah formation, Al Qasim district, Saudi Arabia. Proc. Geol. Assoc. 116, 331–347.
Cohen, K.M., Harper, D.A.T., Gibbard, P.L., 2016. The ICS International Chronostratigraphic Chart. Episodes 12.
Dabard, M.P., Loi, A., Paris, F., Ghienne, J.F., Pistis, M., Vidal, M., 2015. Sea-level curve for the Middle to early Late Ordovician in the Armorican Massif (western France): icehouse third-order glacio-eustatic cycles. Palaeogeogr. Palaeoclimatol. Palaeoecol. 436, 96–111.
Díaz-Martínez, E., Grahn, Y., 2007. Early Silurian glaciation along the western margin of Gondwana (Peru, Bolivia and northern Argentina): palaeogeographic and geodynamic setting. Palaeogeogr. Palaeoclimatol. Palaeoecol. 245, 62–81.
Elaouad-Debbaj, Z., 1984. Chitinozoaires ashgilliens de l'Anti-Atlas (Maroc). Géobios 17, 45–46.
Fensome, R.A., Williams, G.L., Barss, M.S., Freeman, J.M., Hill, J.M., 1990. Acritarchs and fossil prasinophyte: an index to genera, species, intraspecific taxa. A.A.S.P. Contrib. Ser. 25, pp. 1–771.
Fortey, R.A., Cocks, L.R.M., 2013. Late Ordovician global warming, the Boda event. Geology 33, 405–408.
Ghavidel-Syooki, M., 2008. Palynostratigraphy and Palaeogeography of the Upper Ordovician Gorgan Schists (Southeastern Caspian Sea), Eastern Alborz Mountain Ranges, Northern Iran. Comunicações Geológicas 95, 123–155.
Ghavidel-Syooki, M., 2016a. Cryptospore and trilete spore assemblages from the Late Ordovician (Katian–Hirnantian) Ghelli Formation, Alborz Mountain Range, Northeastern Iran: palaeophytogeographic and palaeoclimatic implications. Rev. Palaeobot. Palynol. 231, 48–71.

Ghavidel-Syooki, M., 2016b. Biostratigraphy of acritarchs and chitinozoans in Ordovician strata from the Fazel Abad area, southeastern Caspian Sea, Alborz Mountains, northern Iran: stratigraphic and paleogeographic implications. In: Sorkhabi, R. (Ed.), Tectonic Evolution, Collision, and Seismicity of Southwest Asia: In Honor of Manuel Berberian's Forty-five Years of Research Contributions. 525. Geological Society of America Special Paper:pp. 1–32. http://dx.doi.org/10.1130/2016.2525 (11).

Ghavidel-Syooki, M., Vecoli, M., 2007. Latest Ordovician-early Silurian chitinozoans from the eastern Alborz Mountain Range, Kopet-Dagh region, northeastern Iran: biostratigraphy and paleobiogeography. Rev. Palaeobot. Palynol. 145, 173–192.

Ghavidel-Syooki, M., Winchester-Seeto, T., 2002. Biostratigraphy and Palaeogeography of Late Ordovician chitinozoans from the northeastern Alborz Range, Iran. Rev. Palaeobot. Palynol. 118, 77–99.

Ghavidel-Syooki, M., Winchester-Seeto, T., 2004. Chitinozoan biostratigraphy and palaeogeography of lower Silurian strata (Sarchahan Formation) in the Zagros Basin of southern Iran. Mem. Assn. Austral. Palaeontol. 29, 161–182.

Ghavidel-Syooki, M., Álvaro, J.J., Popov, L., Ghobadi Pour, M., Ehsani, M.H., Suyarkova, A., 2011. Stratigraphic evidence for the Hirnantian (latest Ordovician) glaciation in the Zagros Mountains, Iran. Palaeogeogr. Palaeoclimatol. Palaeoecol. 307, 1–16.

Ghavidel-Syooki, M., Evans, D.H., Ghobadi Pour, M., Popov, L.E., Alvaro, J.J., Rakhmonov, U., Klishevich, I.A., Ehsani, M.H., 2015. Late Ordovician cephalopods, tentaculitides, machaeridians and echinoderms from Kuh-e Faraghan, High Zagros, Iran. Alcheringa 39. http://dx.doi.org/10.1080/03115518.2015.1052677.

Ghienne, J.F., 2003. Late Ordovician sedimentary environments, glacial cycles, and post-glacial transgression in the Taoudeni Basin, West Africa. Palaeogeogr. Palaeoclimatol. Palaeoecol. 189, 117–145.

Ghienne, J.-F., Boumendjel, K., Paris, F., Videt, B., Racheboeuf, P., Ait Salem, H., 2007. The Cambrian–Ordovician succession in the Ougarta Range (western Algeria, North Africa) and interference of the Late Ordovician glaciation on the development of the lower Palaeozoic transgression on northern Gondwana. Bull. Geosci. 82 (3), 183–214.

Gray, J., Boucot, A.J., 1989. Is Moyeria a eugelnoid? Lethaia 22, 447–456.

Greuter, W.F.R., Barrie, H.M., Burdet, W.G., Chaloner, V., DeMoulin, D.L., Hawksworth, P.M., Jφrgensen, J., McNeil, D.H., Nicolson, P.C.S., Trehane, P., 1994. International code of botanical nomenclature (Tokyo Code). Regnum Vegetable. 131. Koeltz Scientific Books, Königstein (389 pp.).

Hammann, W., 1992. The Ordovician trilobites from the Iberian Chains in the province of Aragon, NE-Spain. I. The trilobites of the cystoid limestone (Ashgill series). Beringeria 6, 219.

Heydari, E., 2008. Tectonic versus eustatic controls on supersequences of the Zagros Mountains of Iran. Tectonophysics 451, 56–70.

Hirst, J.P.P., 2015. Ordovician proglacial sediments in Algeria: insights into the controls on hydrocarbon reservoirs in the In Amenas field, Illizi Basin. Geol. Soc. Lond. Spec. Publ. 368, 319–353.

Hirst, J.P.P., Benbakir, A., Payne, D.F., Westlake, I.R., 2002. Tunnel valleys and density flow processes in the upper Ordovician glacial succession, Illizi Basin, Algeria: influence on reservoir quality. J. Pet. Geol. 25, 297–324.

Husseini, M.I., 1990. The Cambro-Ordovician Arabian and adjoining plates: a glacioeustatic model. J. Pet. Geol. 13, 267–288.

Jacobson, S.R., Achab, A., 1985. Acritarch biostratigraphy of the Dicellograptus complanatus graptolite zone from the Vaureal Formation (Ashgillian), Anticosti Island, Quebec, Canada. Palynology 9, 165–198.

Jenkins, W.A.M., 1967. Ordovician Chitinozoa from Shropshire. Palaeontology 10, 436–488.

Jenkins, W.A.M., 1970. Chitinozoa from the Ordovician Sylvan Shale of the Arbuckle Mountains, Oklahoma. Palaeontology 13, 261–288.

Kjellström, G., 1971. Middle Ordovician microplankton from the Grötlingbo, Borehole no.1 in Gotland, Sweden. Sveriges Geologiska Undersökning Serie C. 669, pp. 1–35.

Le Hérissé, A., Paris, F., Steemans, P., 2013. Late Ordovician- earliest Silurian palynomorphs from northern Chad and correlation with contemporaneous deposits of southeastern Libya. Bull. Geosci. 88, 483–504 (10 figures).

Le Hérissé, A., Molyneux, S., Miller, M., 2015. Late Ordovician to early Silurian acritarchs from the Qusaiba-1 shallow core hole, central Saudi Arabia. Rev. Palaeobot. Palynol. 212, 22–59.

Le Heron, D.P., Craig, J., 2008. First-order reconstructions of a Late Ordovician Saharan ice sheet. J. Geol. Soc. 165, 19–29.

Le Heron, D.P., Dowdeswell, J.A., 2009. Calculating ice volumes and ice flux to constrain the dimensions of a 440 Ma North African ice sheet. J. Geol. Soc. Lond. 166, 277–281.

Le Heron, D.P., Sutcliffe, O., Bourgig, K., Craig, J., Visentin, C., Whittington, R., 2004. Sedimentary architecture of Upper Ordovician tunnel valleys, Gargaf Arch, Libya: implications for the genesis of a hydrocarbon reservoir. GeoArabia 9, 137–160.

Le Heron, D.P., Ghienne, J.F., El Houicha, M., Khoukhi, Y., Rubino, J.L., 2007. Maximum extent of ice sheets in Morocco during the Late Ordovician glaciation. Palaeogeogr. Palaeoclimatol. Palaeoecol. 245, 200–226.

Le Heron, D.P., Khoukhi, Y., Paris, F., Ghienne, J.F., Le Hérissé, A., 2008. Black shale, grey shale, fossils and glaciers: anatomy of the Upper Ordovician–Silurian succession in the Tazzeka Massif of eastern Morocco. Gondwana Res. 14, 483–496.

Li, J., Wicander, R., Yan, K., Zhu, H., 2006. An Upper Ordovician acritarch and prasinophyte assemblage from Dawangou, Xinjiang, northwestern China: biostratigraphic and palaeogeographic implications. Rev. Palaeobot. Palynol. 139, 97–128.

Loeblich Jr., A.R., 1970. Morphology, ultrastructure and distribution of Paleozoic acritarchs. Proc. Am. Paleontol. Conv. Chicago, pp. 705–788.

Loeblich Jr., A.R., Tappan, H., 1978. Some Middle and Late Ordovician microphytoplankton from central North America. J. Paleontol. 52, 1233–1287.

Loi, A., Ghienne, J.F., Dabard, M.P., Paris, F., Botquelen, A., Christ, N., Elaouad-Debbaj, Z., Gorini, A., Vidal, M., Videt, B., Destombes, J., 2010. The Late Ordovician glacioeustatic record from a high-latitude storm-dominated shelf succession: the Bou Ingarf section (Anti-Atlas, Southern Morocco). Palaeogeogr. Palaeoclimatol. Palaeoecol. 296, 332–358.

McClure, H.A., 1978. Early Paleozoic glaciation in Arabia. Palaeogeogr. Palaeoclimatol. Palaeoecol. 25, 315–326.

McClure, H.A., 1988. Chitinozoan and acritarch assemblages, stratigraphy and biogeography of the early Palaeozoic of Northwest Arabia. Rev. Palaeobot. Palynol. 56, 41–60.

McGillivray, J.G., Husseini, M.I., 1992. The Paleozoic petroleum geology of Central Arabia. AAPG Bull. 76, 1473–1490.

Melvin, J., 2015. Lithostratigraphy and depositional history of Upper Ordovician and lowermost Silurian sediments recovered from the Qusaiba-1 shallow core hole, Qasim region, central Saudi Arabia. Rev. Palaeobot. Palynol. 212, 3–21.

Melvin, J., Sutcliffe, O.E., Ferebee, T., 2003. Origin and sedimentary infill of an Upper Ordovician (Ashgillian), glacial paleovalley near Tabuk, Northwest Saudi Arabia. Abstracts, 7th GEO Middle East Conference and Exhibition. Geol. Soc. London, p. 90051 (October 2003).

Miller, M.A., Mansour, H.A.R., 2007. Preliminary palynological investigation of Saudi Arabian Upper Ordovician glacial sediments. Rev. Micropaleontol. 50, 17–26.

Molyneux, S.G., Paris, F., 1985. Late Ordovician palynomorphs. In: Thusu, B., Owens, B. (Eds.), Palynostratigraphy of North-East Libya. J. Micropalaeontol. 4(1), pp. 11–26.

Monaldi, C.R., Boso, M.A., 1987. Dalmanitina (Dalmanitina) subandina nov. sp. (Trilobita) en la Formaci on Zapla del norte argentino. Actas 4° Congreso Latinoamericano de Paleontología, Santa Cruz de la Sierra. 1, pp. 149–157.

Monod, O., Kozlu, H., Ghienne, J.F., Dean, W.T., Günay, Y., Le Hérissé, A., Paris, F., Robardet, M., 2003. Late Ordovician glaciation in southern Turkey. Terra Nova 15, 249–257.

Nestor, V., 1980. New chitinozoan species from the lower Llandoverian of Estonia. Eesti NSV Tead. Akad. Toim. 29, 98–107.

Nestor, V., 1994. Early Silurian chitinozoans of Estonia and northern Latvia. Acad. Ther. 4 (163 pp.).

Oulebsir, L., Paris, F., 1995. Chitinozoaires Ordoviciens du Sahara algérien: biostratigraphie et affinités paléogéographiques. Rev. Palaeobot. Palynol. 86, 49–68.

Paris, F., 1990. The Ordovician biozones of the North Gondwana Domain. Rev. Palaeobot. Palynol. 66, 181–209.

Paris, F., 1996. Chitinozoan biostratigraphy and palaeoecology. In: Jansonius, J., McGregor, D.C. (Eds.), Palynology: Principles and Applications. vol. 2. American Association of Stratigraphic Palynologists Foundation, pp. 531–552.

Paris, F., Elaouad-Debbaj, Z., Jaglin, J.C., Massa, D., Oulebsir, L., 1995. Chitinozoans and Late Ordovician Glacial events on Gondwana. In: Cooper, J.D., Droser, M.L., Finney, S. (Eds.), Ordovician Odyssey. Seventh International Symposium on Ordovician System, Las Vegas. The Pacific Section Society for Sedimentary Geology (SEPM), Fullerton, pp. 171–176.

Paris, F., Grahn, Y., Nestor, Y., Lakova, I., 1999. A revised chitinozoan classification. J. Paleontol. 73 (4), 549–570.

Paris, F., Bourahrouh, A., Le Hérissé, A., 2000a. The effects of the final stages of the Late Ordovician glaciation on marine palynomorphs (chitinozoans, acritarchs, leiospheres) in well Nl-2 (NE Algerian Sahara). Rev. Palaeobot. Palynol. 113, 87–104.

Paris, F., Verniers, J., Al-Hajri, S., 2000b. Ordovician chitinozoans from Central Saudi Arabia. In: Al-Hajri, S., Owens, B. (Eds.), Stratigraphic Palynology of the Palaeozoic of Saudi Arabia. GeoArabia Special Publication No. 1, pp. 42–56.

Paris, F., Le Hérissé, A., Monod, O., Kozlu, H., Ghienne, J.F., Dean, W.T., Vecoli, M., Gunay, Y., 2007. Ordovician chitinozoans and acritarchs from southern and southeastern Turkey. Rev. Micropaleontol. 50, 81–107.

Paris, F., Verniers, J., Miller, M.A., Al-Hajri, S., Melvin, J., Wellman, C.H., 2015. Late Ordovician–earliest Silurian chitinozoans from the Qusaiba-1 core hole (North Central Saudi Arabia) and their relation to the Hirnantian glaciation. Rev. Palaeobot. Palynol. 212, 60–84.

Powell, J.H., Kahlil, B.M., Masri, A., 1994. Late Ordovician–Early Silurian glaciofluvial deposits preserved in palaeovalleys in South Jordan. Sediment. Geol. 89, 303–314.

Raevskaya, E., Dronov, A., 2014. Late Ordovician acritarchs from the Tungus basin, Siberia platform. Estonian J. Earth Sci. 63 (4), 300–304.

Senalp, M., Al-Laboun, A., 2000. New evidence on the Late Ordovician glaciation in Central Saudi Arabia. Saudi Aramco J. Technol. 11–40 (Spring).

Staplin, F.L., Jansonius, J., Pocock, S.A.J., 1965. Evaluation of some acritarcheous hystrichosphere genera. N. Jb. Geol. Paläont. (Abh.) 123, 167–201.

Sutcliffe, O.E., Dosdeswell, J.A., Whittington, R.J., Theron, J.N., Craig, J., 2000. Calibrating the Late Ordovician glaciation and mass extinction by the eccentricity cycles of Earth's orbit. Geology 28, 967–970.

Torsvik, T.H., Cocks, L.R.M., 2009. The lower Palaeozoic palaeogeographical evolution of the northeastern and eastern peri-Gondwanan margin from Turkey to New Zealand. In: Bassett, M.G. (Ed.), Early Palaeozoic Peri-Gondwana Terranes: New Insights From Tectonics and Biogeography. 325. Geol. Soc., London, Spec. Publ., pp. 3–21.

Turner, B.R., Makhlouf, I.M., Armstrong, H.A., 2005. Late Ordovician (Ashgillian) glacial deposits in southern Jordan. Sediment. Geol. 181, 73–91.

Van Nieuwenhove, N., Vanderbroucke, T.R.A., Verniers, J., 2006. The Chitinozoan biostratigraphy of the Upper Ordovician Greenscoe section, southern Lake District, UK. Rev. Palaeobot. Palynol. 139, 151–169.

Vandenbroucke, T.R.A., 2008. Upper Ordovician Chitinozoans From the Type Area in the U.K. Monograph Palaeontol. 161. Soc. Lond, pp. 1–113.

Vandenbroucke, T., Gabbot, S.E., Paris, F., Aldridge, R.J., Theron, J.N., 2009. Chitinozoans and the age of the Soom Shale, Ordovician black shale Lagerstatte, South Africa. J. Micropalaeontol. 28, 53–66.

Vanmeirhaeghe, J., 2006. Chitinozoan biostratigraphy of the Upper Ordovician of Faulx-les-Tombes (central Condroz Inlier, Belgium). Rev. Palaeobot. Palynol. 139, 171–188.

Vaslet, D., 1990. Upper Ordovician glacial deposits in Saudi Arabia. Episodes 13 (3), 147–161.

Vecoli, M., Le Hérissé, A., 2004. Biostratigraphy taxonomic diversity and patterns of morphological evolution of Ordovician acritarchs (organic-walled microphytoplankton) from the northern Gondwana margin in relation to palaeoclimatic and palaeogeographic changes. Earth-Sci. Rev. 67, 267–311.

Vennin, E., Alvaro, J.J., Villas, E., 1998. High-latitude pelmatozoan-bryozoan mud-mounds from the late Ordovician northern Gondwana platform. Geol. J. 33, 121–140.

Verniers, J., Nestor, V., Paris, F., Dufka, P., Sutherland, S., Van Grootel, G., 1995. A global chitinozoan biozonation for the Silurian. Geol. Mag. 132, 651–666.

Videt, B., Paris, F., Rubino, J.L., Boumendjel, K., Dabard, M.P., Loi, A., Ghienne, J.F., Marante, A., Gorini, A., 2010. Biostratigraphically calibration of third order Ordovician sequences on the northern Gondwana platform. Palaeogeogr. Palaeoclimatol. Palaeoecol. 296, 359–375.

Villas, E., Vennin, E., Alvaro, J.-J., Hammann, W., Herrera, Z.A., Piovano, E.L., 2002. The Late Ordovician carbonate sedimentation as a major triggering factor of the Hirnantian glaciation. Bull. Soc. Geol. Fr. 173, 569–578.

Webby, B.D., Cooper, R.A., Bergström, S.M., Paris, F., 2004. Stratigraphic framework and time slices. In: Webby, B.D., Paris, F., Droser, M.L., Percival, I.G. (Eds.), The Great Ordovician Biodiversification Event. Columbia University Press, New York, pp. 41–47.

Wicander, R., Playford, G., Robertson, E.B., 1999. Stratigraphic and Palaeogeographic significance of an Upper Ordovician acritarch flora from the Maquoketa shale, northeastern Missouri, U.S.A. Paleontol. Soc. Mem. 51, 1–38.

Wood, G.D., Turnau, E., 2001. New Devonian coenobial chlorococcales (Hydrodictyaceae) from the Holy Cross Mountains and Radom-Lublin region of Poland: their palaeoenvironmental and sequence stratigraphic implications. In: Goodman, D.K., Clarke, R.T. (Eds.), Proceedings of the IX International Palynological Congress Houston, Texas, USA. 1996. American Association of Stratigraphic Palynologists Foundation, pp. 53–63.

Zalasiewicz, J.J., Rushton, A., Vandenbroucke, T., Verniers, J., Stone, P., Floyd, J., 2004. Submission of Hartfell Score (South Scotland) as a GSSP for the base of the middle stage of the Upper Ordovician series. Report for the ISOS GSSP Discussion Site http://www.ordovician.cn (22 pp., 1 pl.).